7th IAA Planetary Defense Conference

26-30 April 2021, Online Event

Hosted by UNOOSA in collaboration with ESA

Session 9b: Impact Effects

Chairs: Patrick Michel | Angela Stickle | Megan Syal

Presenters: J. Pearl | M. Berger | T. Titus |
C. B. Senel | J. Dotson

SPH Simulation of Bolide Entry

7th IAA Planetary Defense Conference

April 2021

Jason Pearl, Cody Raskin & Michael Owen

Lawrence Livermore National Laboratory

LLNL-PRES-821484

This work was performed under the auspices of the U.S. Department of Energy by Lawrence Livermore National Laboratory under Contract DE-AC52-07NA27344. Lawrence Livermore National Security, LLC

Airburst Events

Airburst Events

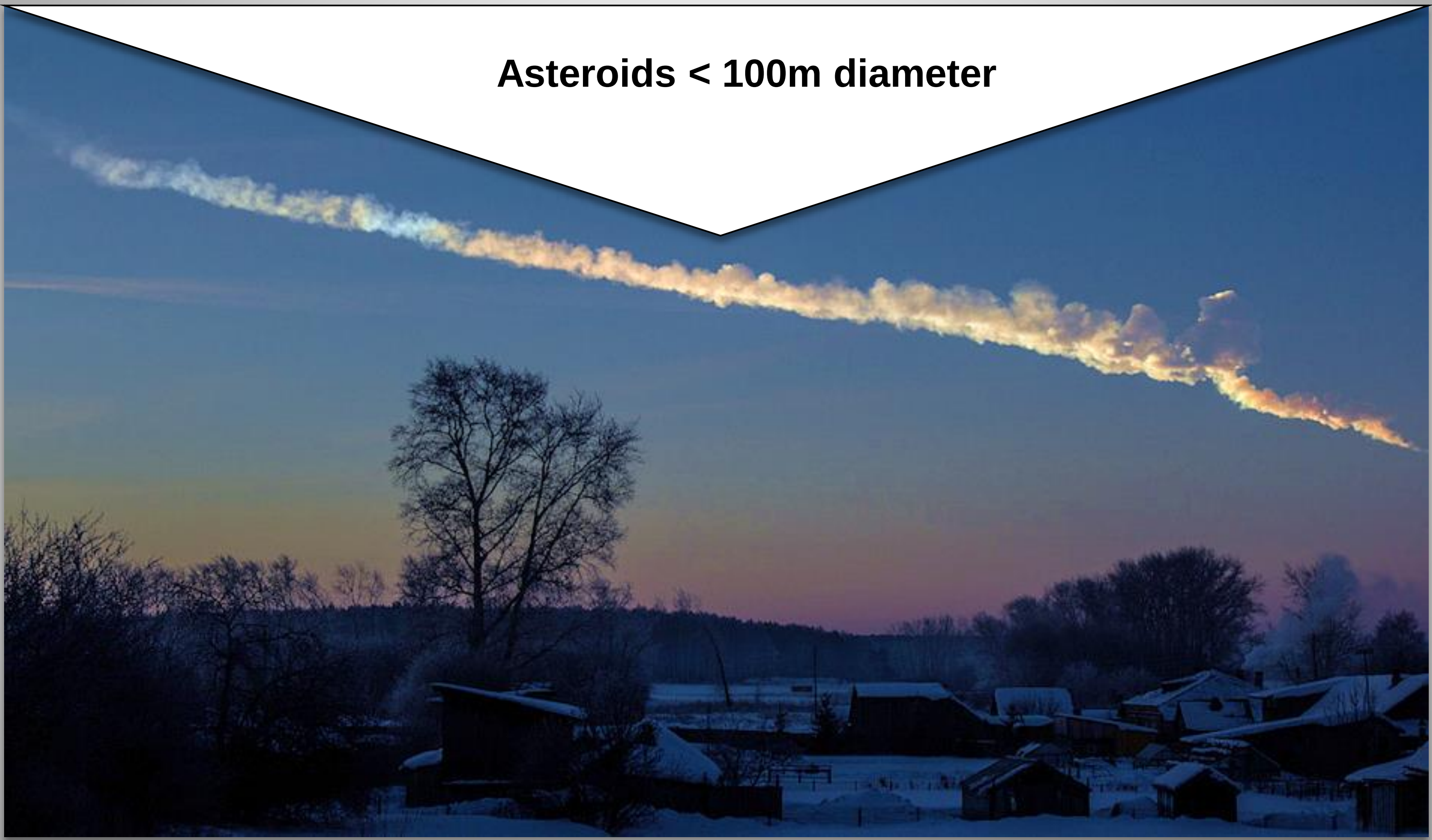

Airburst Events

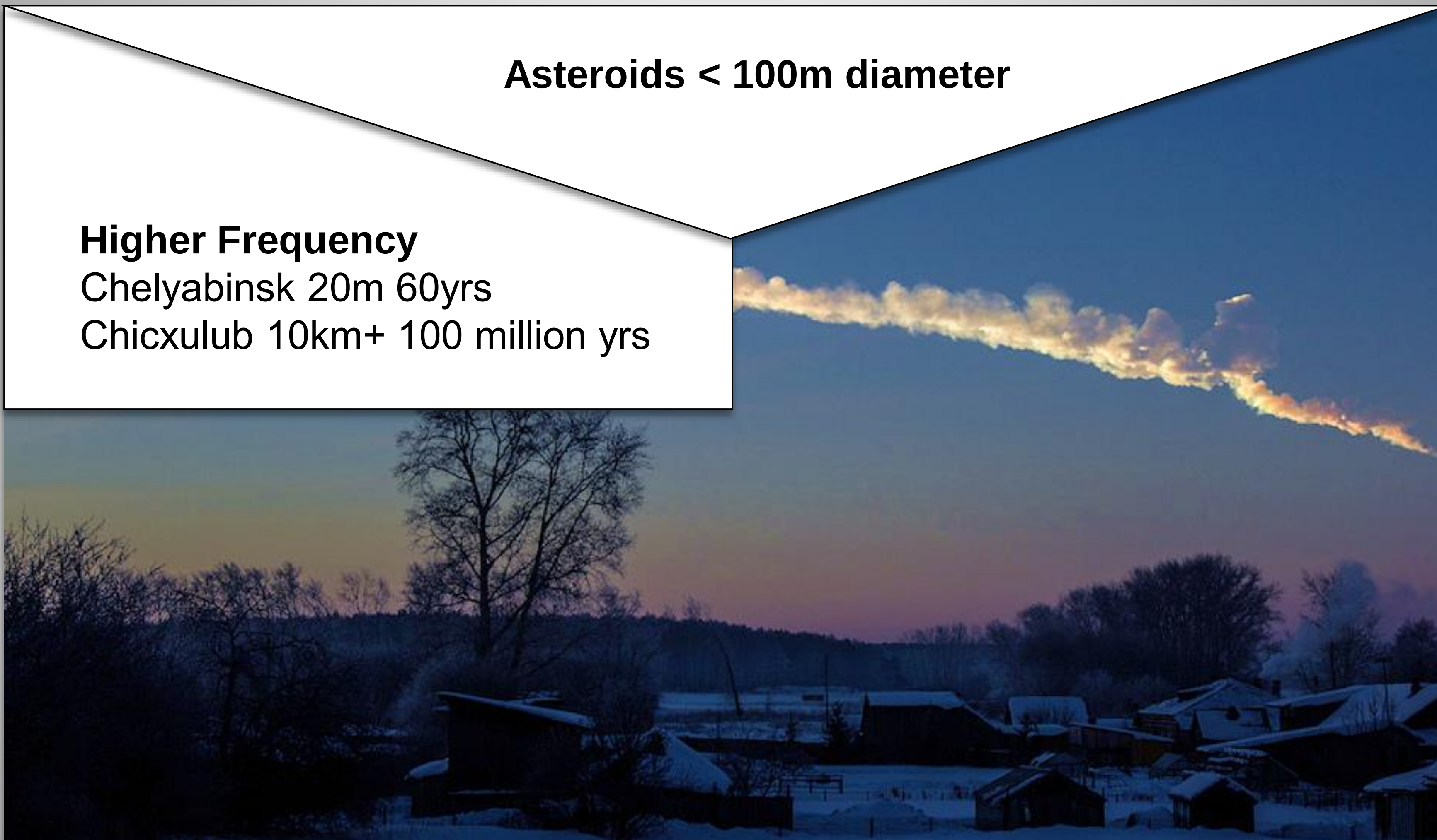

Asteroids < 100m diameter

Higher Frequency
Chelyabinsk 20m 60yrs
Chicxulub 10km+ 100 million yrs

Airburst Events

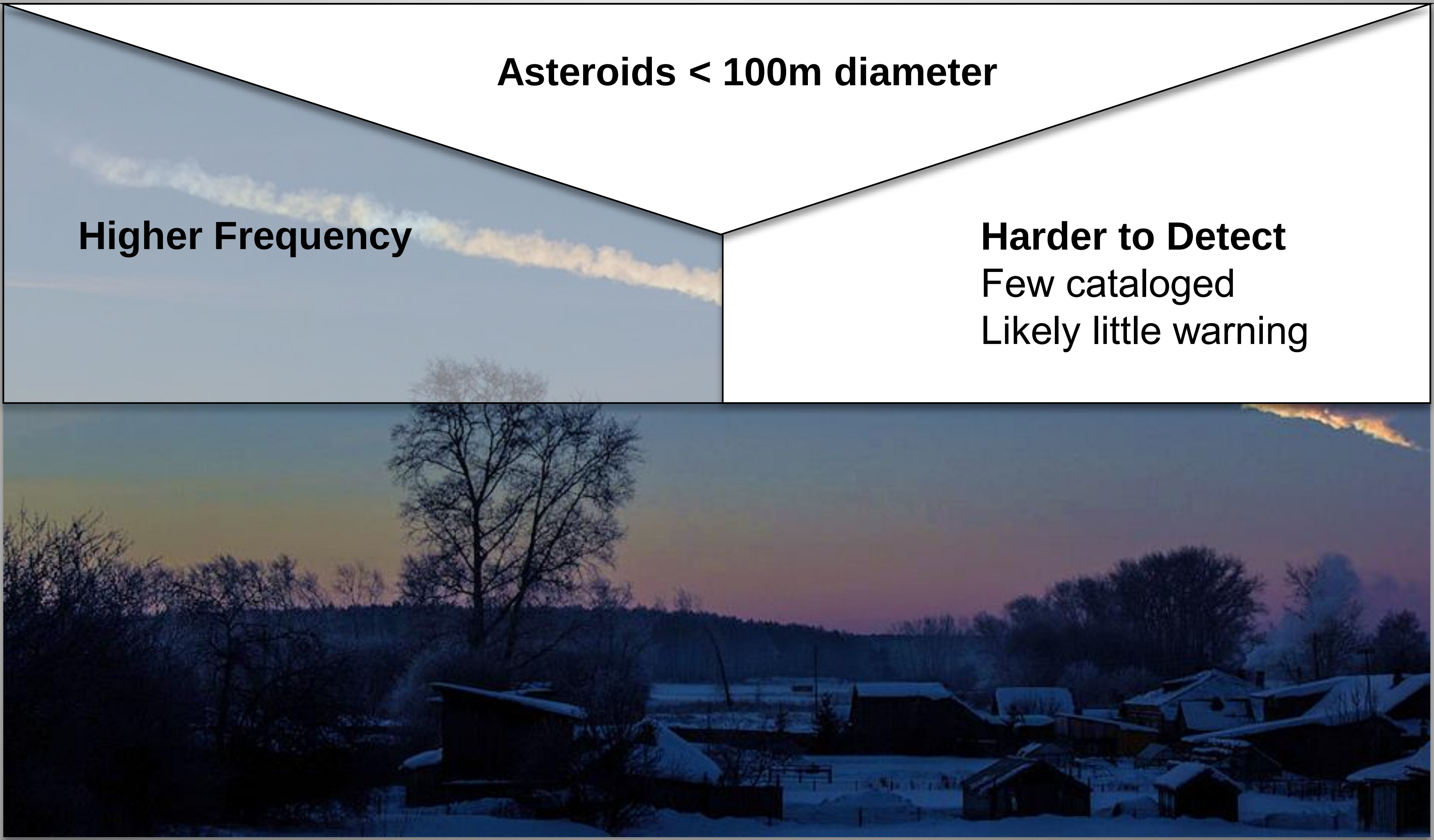

Airburst Events

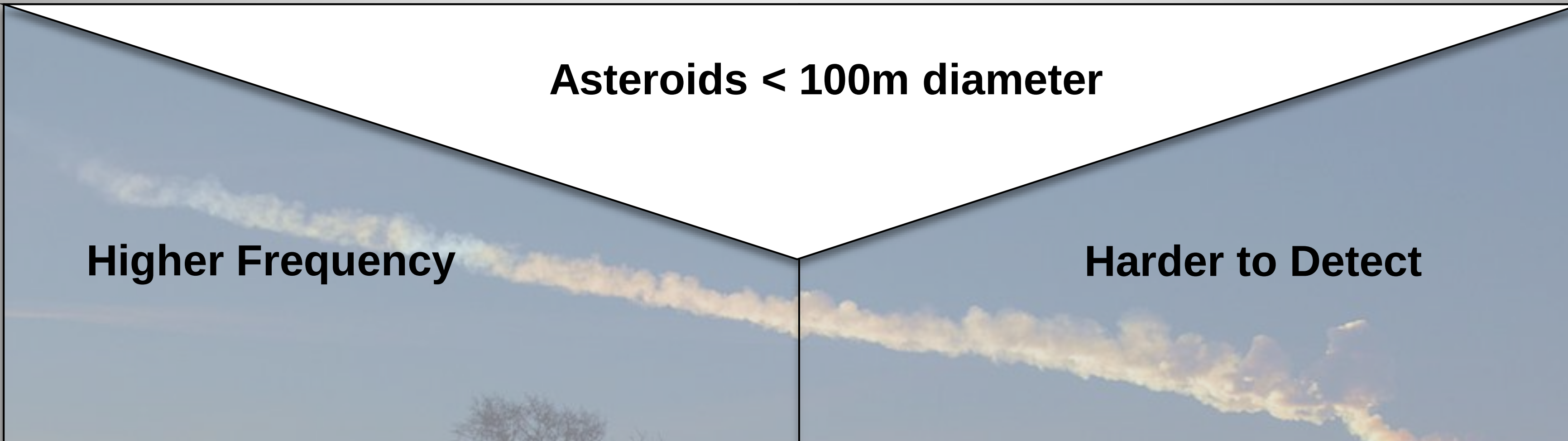

Asteroids < 100m diameter

Higher Frequency

Harder to Detect

Evacuate / Shelter in place?
Prepare infrastructure?
Scale of emergency response?
Scale of financial relief?

Airburst Events

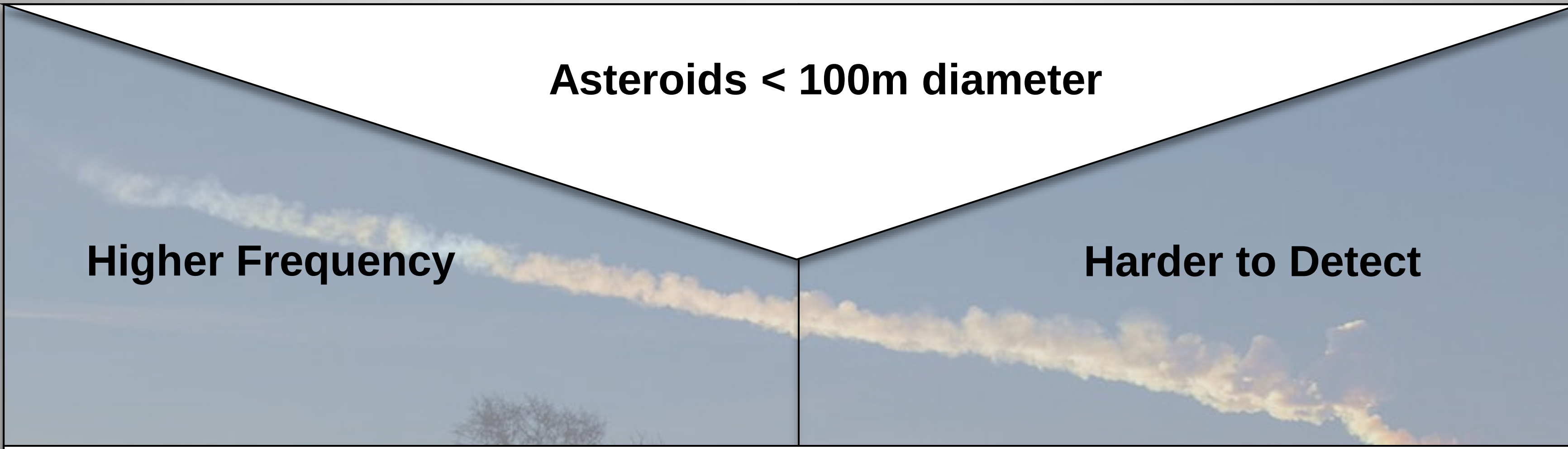

Evacuate / Shelter in place?
Prepare infrastructure?
Scale of emergency response?
Scale of financial relief?

yield?
Height of burst?
Geometry of burst?

Smoothed Particle Hydrodynamics

Summary: Lagrangian meshless method, computational nodes interact with a dynamic neighbor set

Why SPH for Bolides?

- Naturally handles large deformations and interface tracking
- energy/momentum conservation
- Complement grid-code results

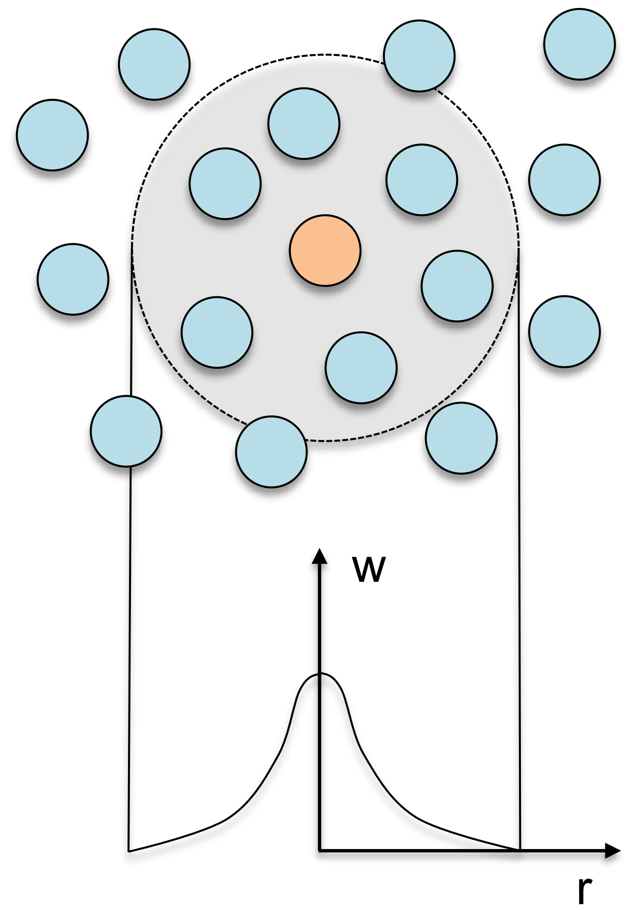

Physics

- 2D Planar
- Euler equations
  - No radiation
  - No heat transfer
  - Zero-strength
- Tillotson EOS for granite
- Gamma-Gas law for air ($\gamma = 1.4$)

Role of Hydrodynamic Instabilities

- Coupled instabilities
  - Rayleigh-Taylor
  - Kelvin-Helmholtz

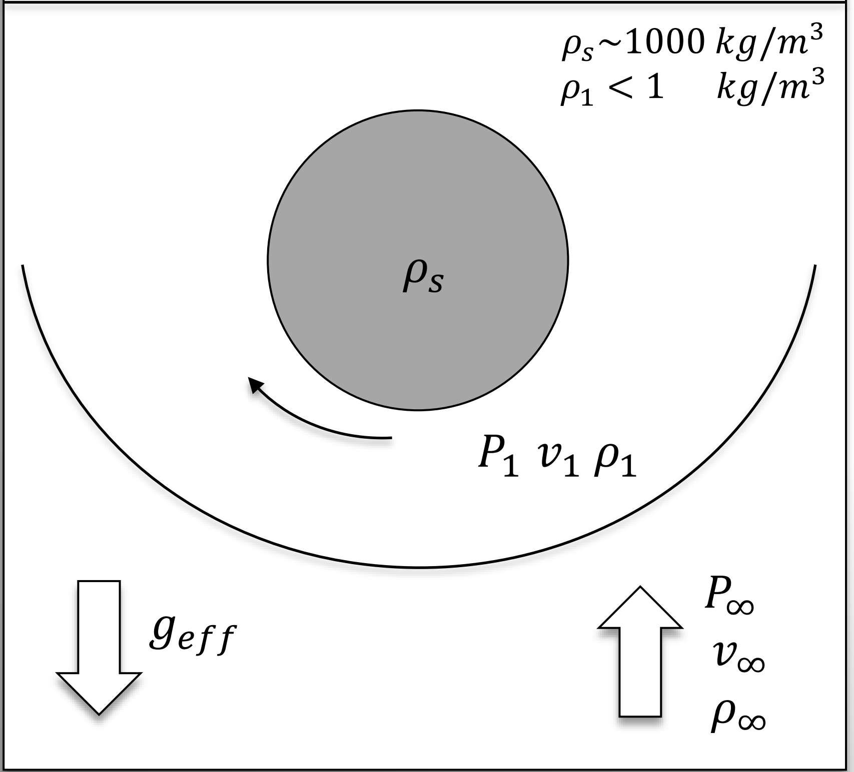

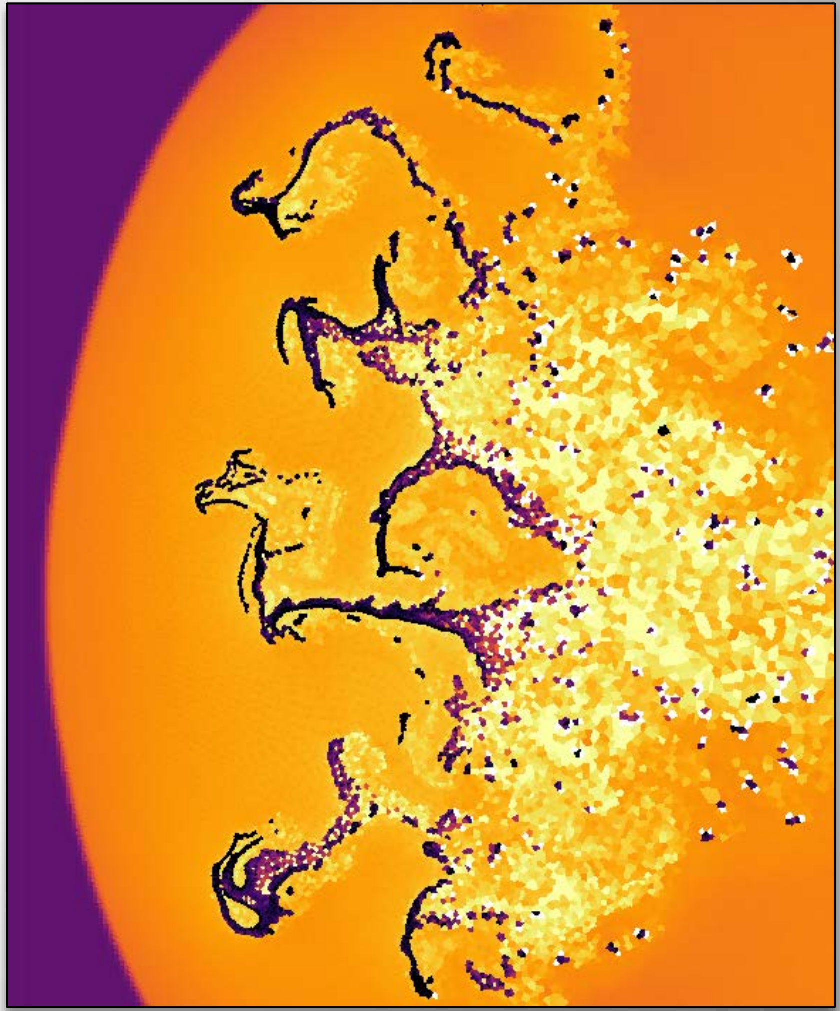

Role of Hydrodynamic Instabilities

- Coupled instabilities
  - Rayleigh-Taylor
  - Kelvin-Helmholtz

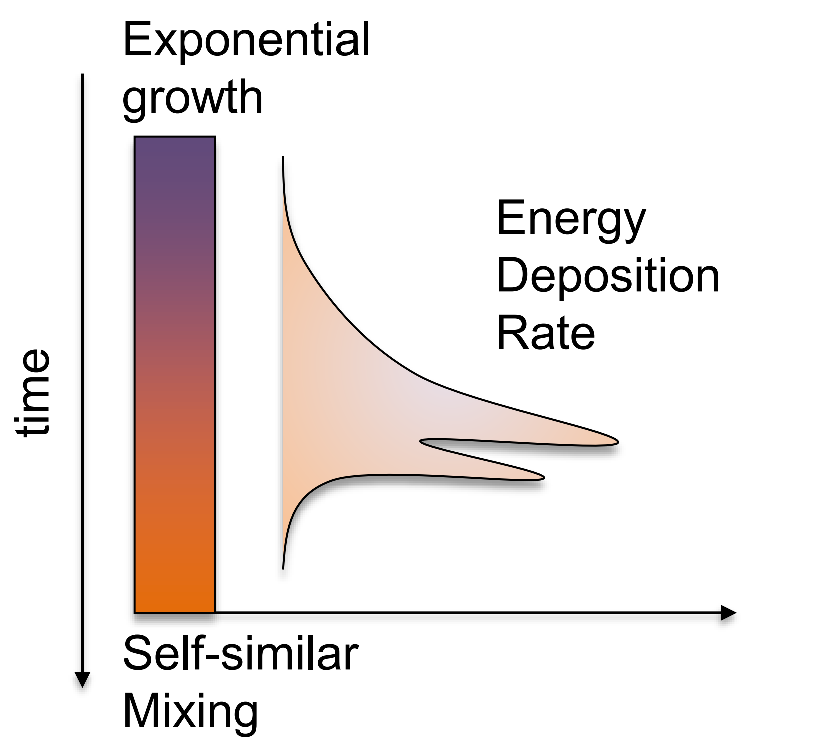

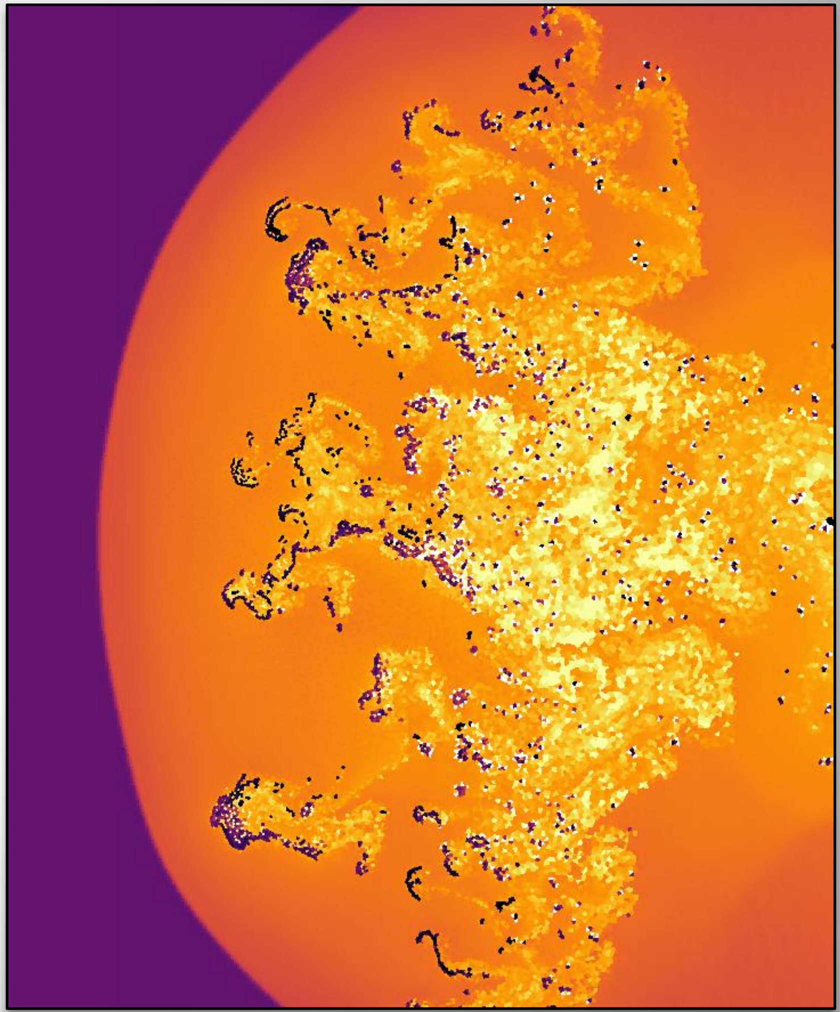

Sensitive Dependence on Initial Conditions

- Strengthless
- ρ = 2.68 g / cc
- Initial velocity = 1.5 km / sec
- Radius = 17.5 m

- 6 perturbed cases run
- Node distribution of bolide rotated to introduce perturbation
- [0.5,1.0,1.5, 2.0, 2.5, 3.0] radians

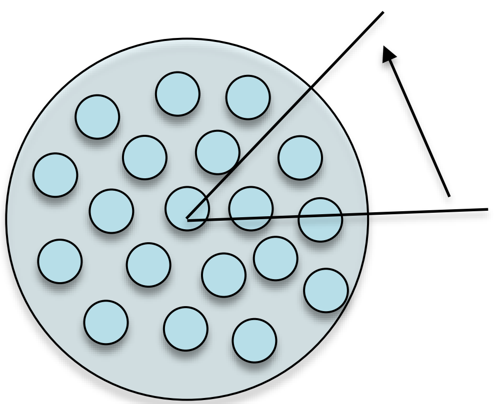

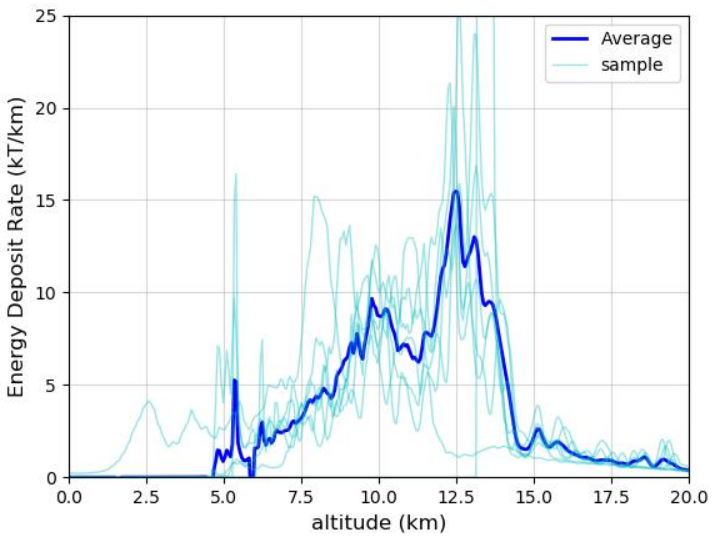

Sensitive Dependence on Initial Conditions

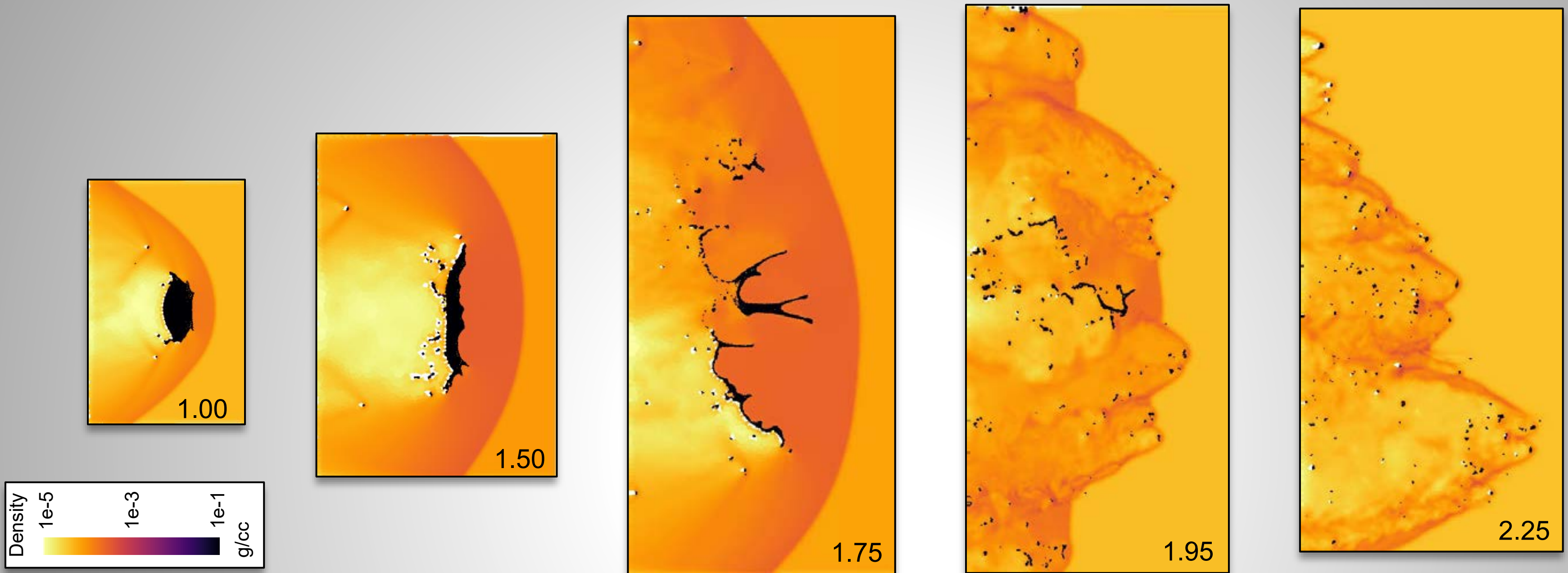

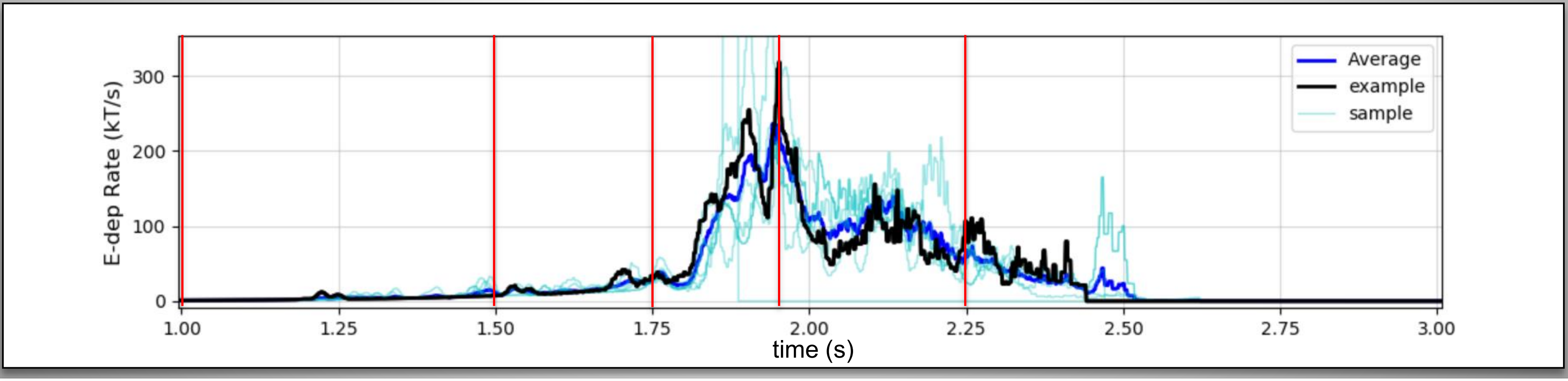

Effects of Surface Perturbations

- Strengthless
- ρ = 2.68 g / cc
- v0= 15.0 km / sec
- Radius ~ 17.5* m
- Constant mass
- Sinusoidal surface perturbations
- Amplitude = 0.1 Radius
- Plots averaged over 6 perturbed runs

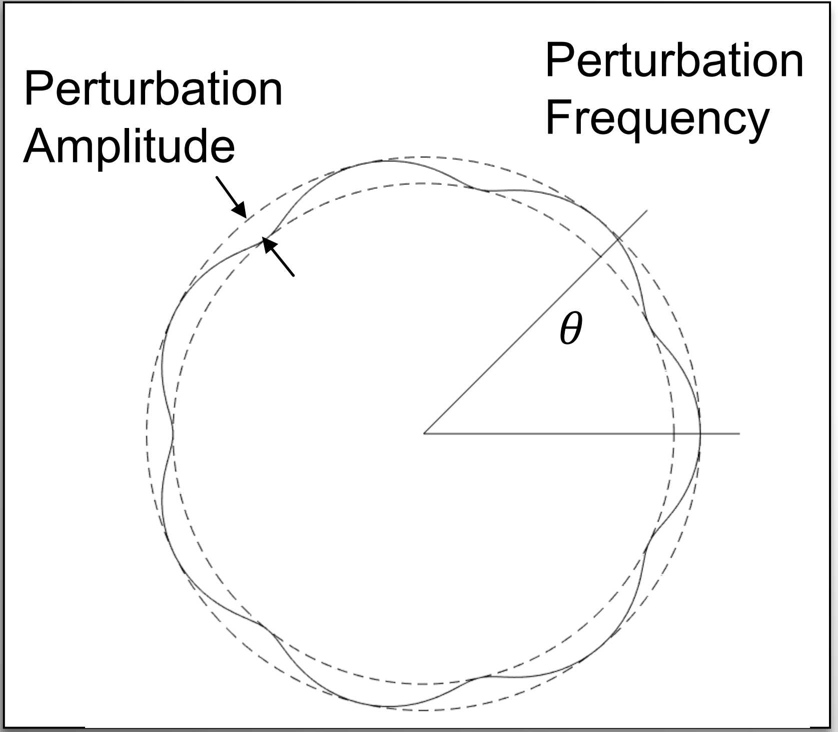

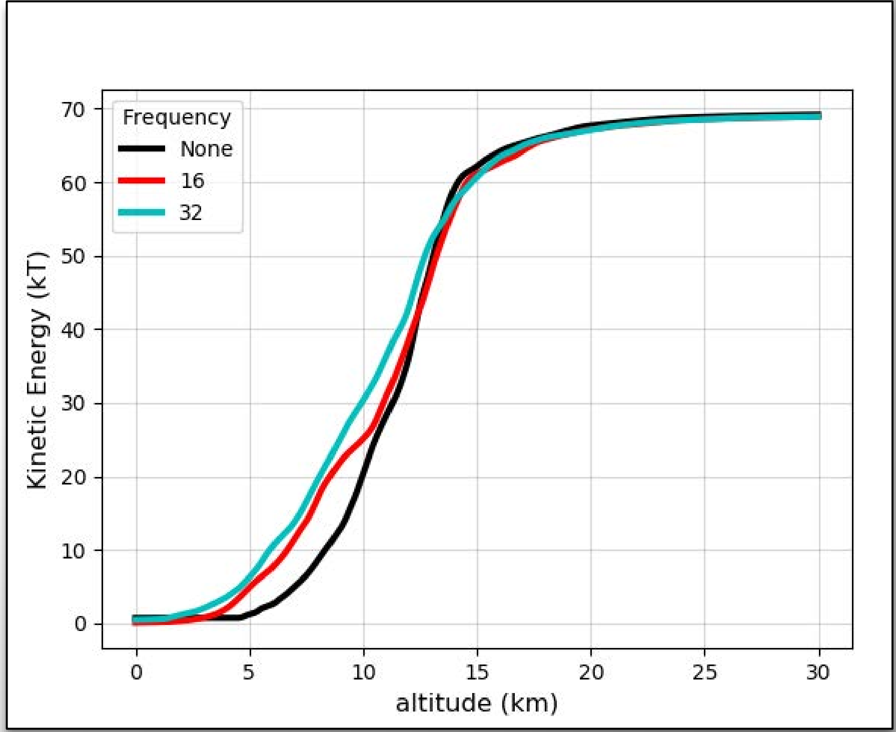

Effects of Surface Perturbations

- Strengthless
- ρ = 2.68 g / cc
- v0= 15.0 km / sec
- Radius ~ 17.5* m
- Constant mass
- Sinusoidal surface perturbations
- Amplitude = 0.1 Radius
- Plots averaged over 6 perturbed runs

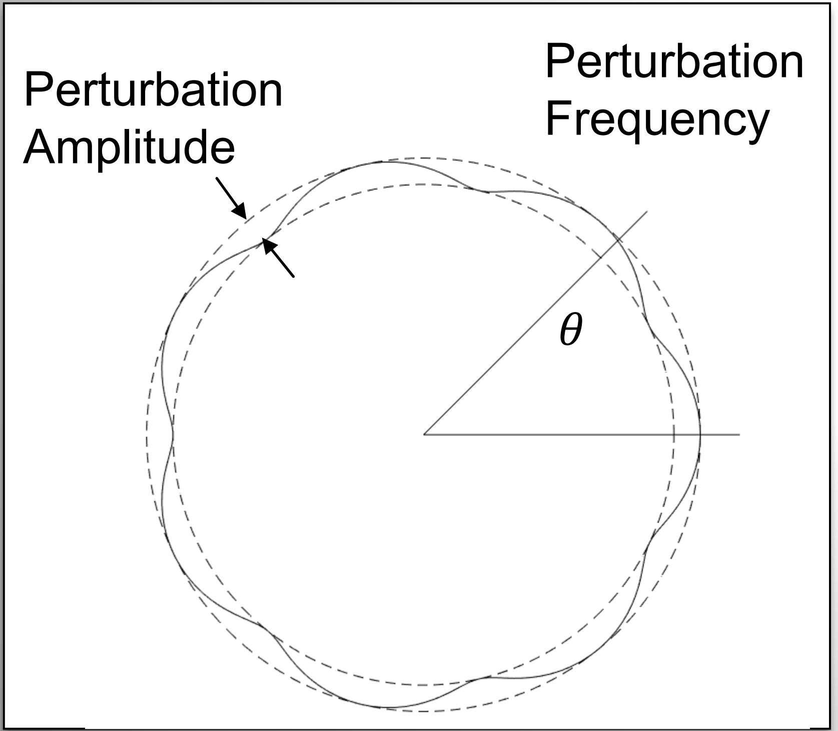

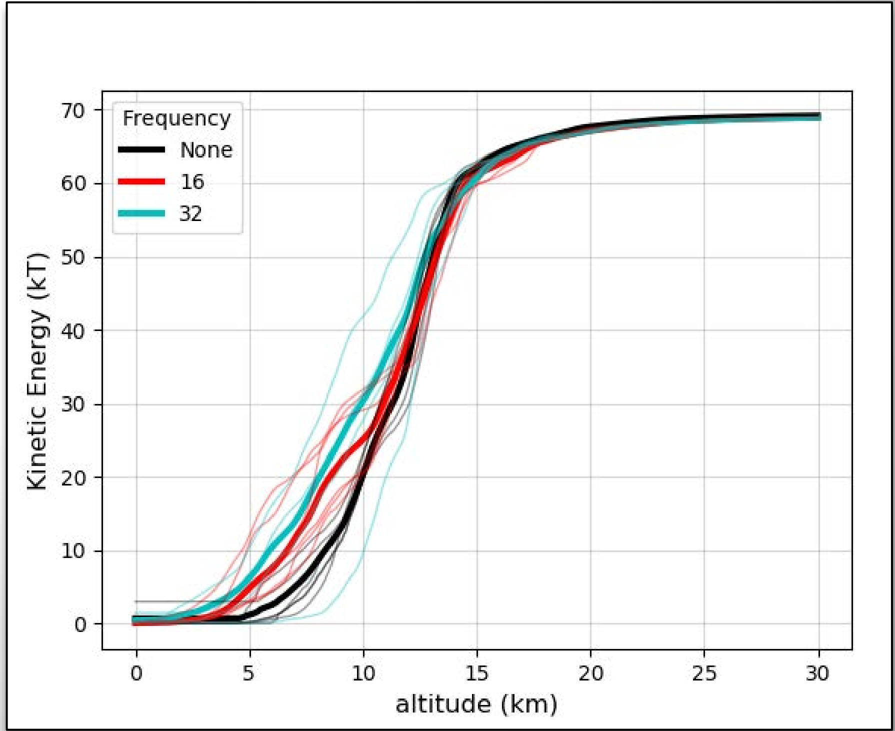

Effects of Surface Perturbations

- Strengthless
- ρ = 2.68 g / cc
- v0= 15.0 km / sec
- Radius ~ 17.5* m
- Constant mass
- Sinusoidal surface perturbations
- Amplitude = 0.1 Radius
- Plots averaged over 6 perturbed runs

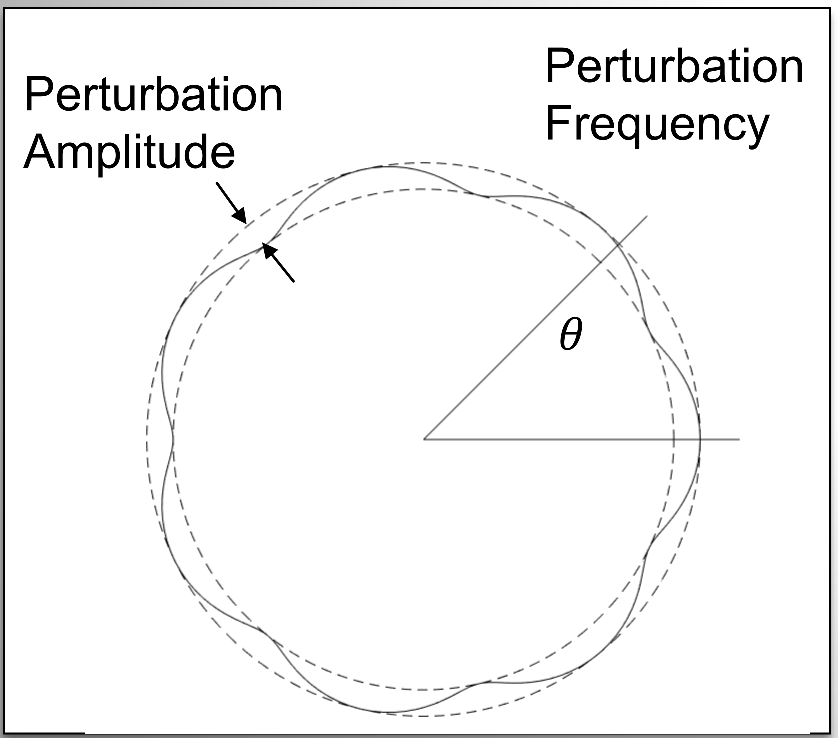

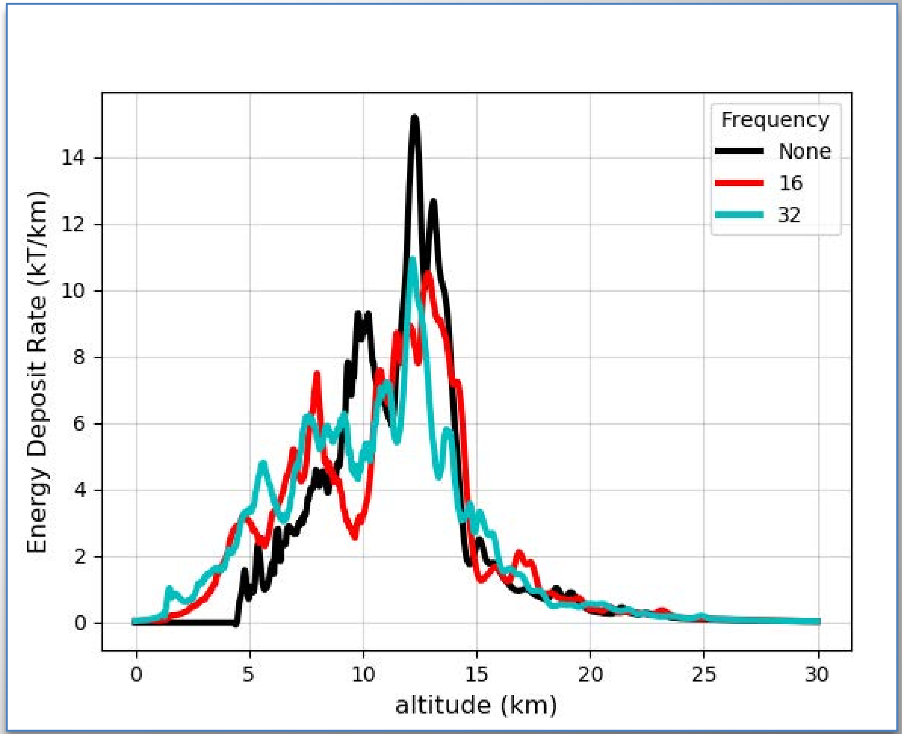

Conclusions

- **Sensitive dependence on initial conditions responsible for considerable spread in results.**
- **Surface perturbations flatten the curve?**
  - On average, cases with surface perturbations deposited energy at low altitudes with smaller peaks.
  - Variation in averages smaller than SDIC variation.

SPH Simulation of Bolide Entry

7th IAA Planetary Defense Conference

April 2021

Jason Pearl, Cody Raskin & J. Michael Owen

Lawrence Livermore National Laboratory

LLNL-PRES-821484

This work was performed under the auspices of the U.S. Department of Energy by Lawrence Livermore National Laboratory under Contract DE-AC52-07NA27344. Lawrence Livermore National Security, LLC

Resolution

- Strengthless
- ρ = 2.68 g / cc
- v0= 1.5 km / sec
- Radius = 17.5 m

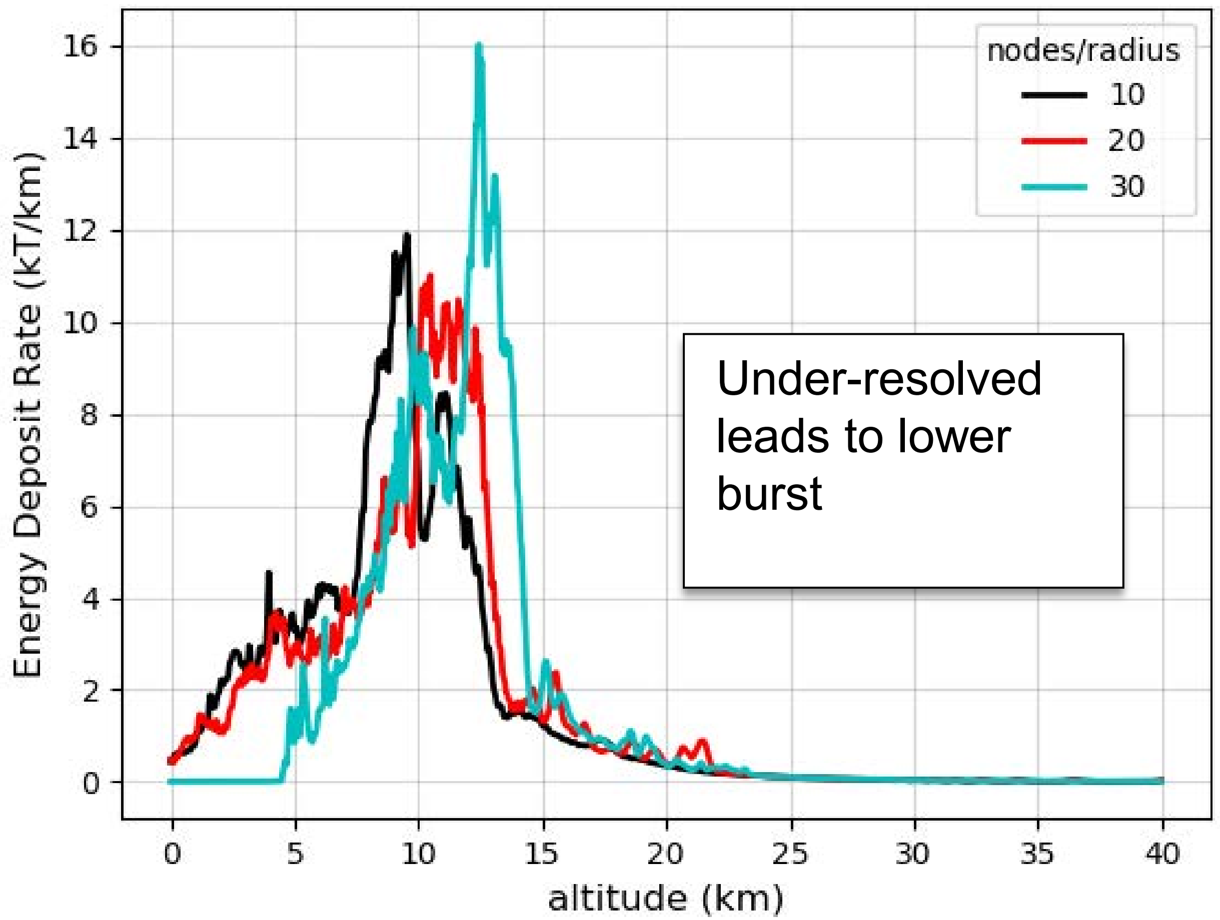

Under-resolved leads to lower burst

*averages for 6 perturbed runs shown in plots

Reference

Korycansky, D.G. and Zahnle, K.J., Mac Law, M.M “High-resolution simulations of the impacts of asteroids into the venusian atmosphere” Icarus, 146, 387-403, 2000.

Towards Adaptive Simulation of Dispersive Tsunami Propagation from an Asteroid Impact

Marsha J. Berger
New York University
Flatiron Institute

Randall J. LeVeque
Emeritus, University of Washington
Visiting Professor, Tohoku University
HyperNumerics LLC

Supported in part by the NASA Asteroid Threat Assessment Project
www.nasa.gov/planetarydefense

Tsunami Propagation

Overview:

- Impact tsunamis have shorter wavelengths than earthquake tsunamis; shallow water model not appropriate
- For ocean-scale propagation want depth-averaged velocities, reducing simulation from $3 \longrightarrow 2$ dimensions
- Boussinesq models include dispersion, need elliptic solve each time step. (This work uses Madsen and Shaffer).

Still need AMR:

- In deep ocean only need resolution of kilometers
- For coastal inundation want resolution of meters

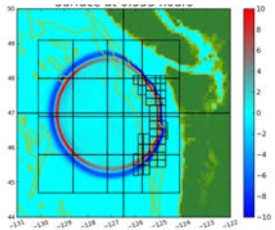

Strategy: Boussinesq in deep ocean, switch to SWE near coast

GeoClaw Software www.geoclaw.org

Based on Clawpack (www.clawpack.org)

- 2d library for depth-averaged flows over topography.
- Handles dry cells where depth $= 0$.
- Well-balanced Riemann solvers for small amplitude waves on ocean at rest.
- Well balancing and dry cells in conjunction with adaptive refinement.
- Well validated for earthquake-generated tsunamis.
- Other applications:
  Debris flows (Dave George, USGS — D-CLAW)
  Storm surge (Kyle Mandli, Columbia)
  Dam breaks / river floods (DG, M. Turzewski, UW,
  D. Calhoun, Boise State – ForestClaw)

Deep Ocean Assessment and Reporting of Tsunamis

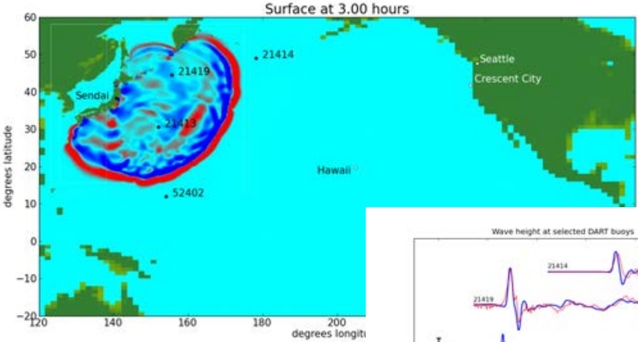

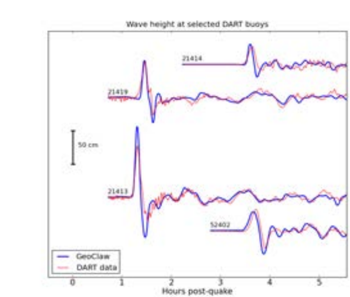

Deep Ocean Assessment and Reporting of Tsunamis

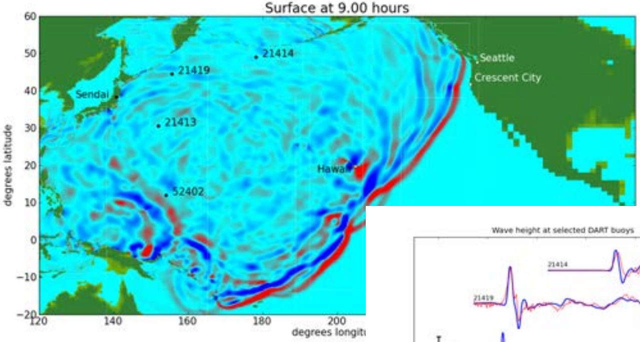

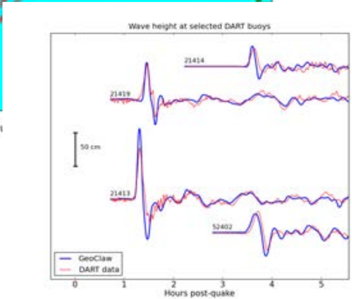

Asteroid Impact Tsunami – Static crater test case

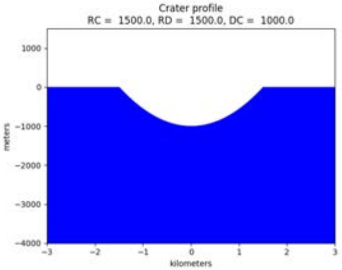

Our tests used the crater with no lip as initial data.

Depth of crater: 1000 m, Depth of ocean: 4000 m.

Initial conditions for 2D Boussinesq:

Full 3D multi-physics hydrocode (ALE3D) was run in 2D axisymmetric mode for this simplified initial condition.

(Darrel Robertson, NASA Ames Research Center).

Asteroid Impact Tsunami – Static crater test case

Surface at $t = 251$ seconds transferred as radially-symmetric initial data for depth-averaged Boussinesq.

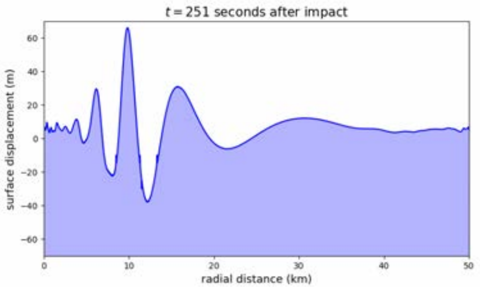

Impact placed ≈ 150 km off Washington coast.

Grays Harbor

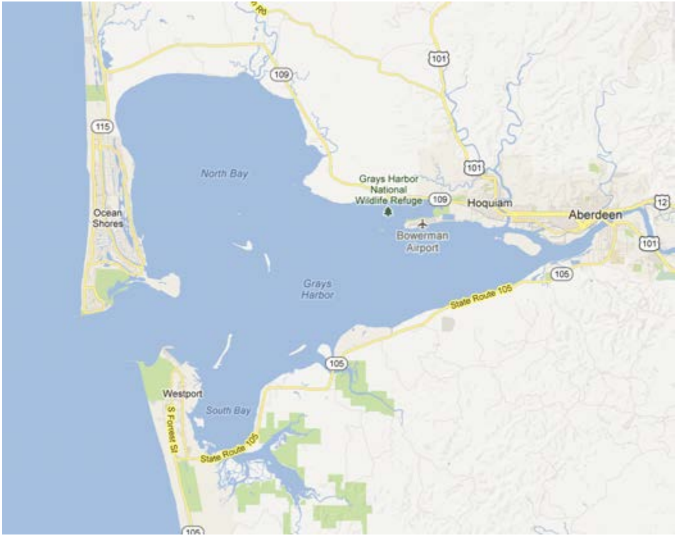

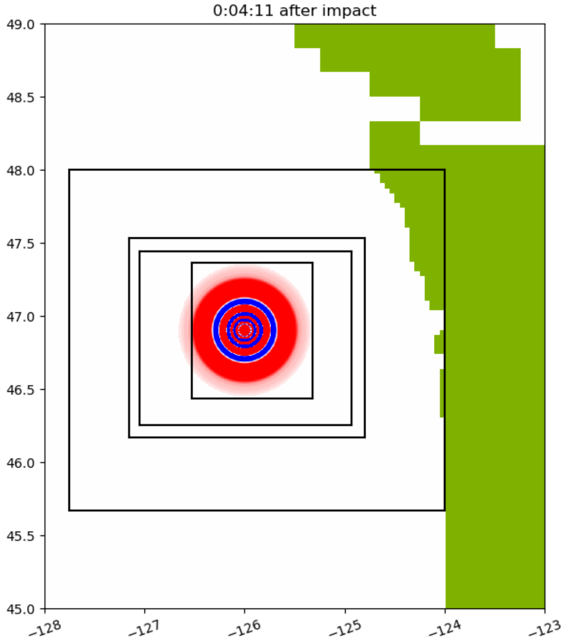
0:04:11 after impact
49.0
48.5
48.0
47.5
47.0
46.5
46.0
45.5
45.0
−128
−127
−126
−125
−124
−123

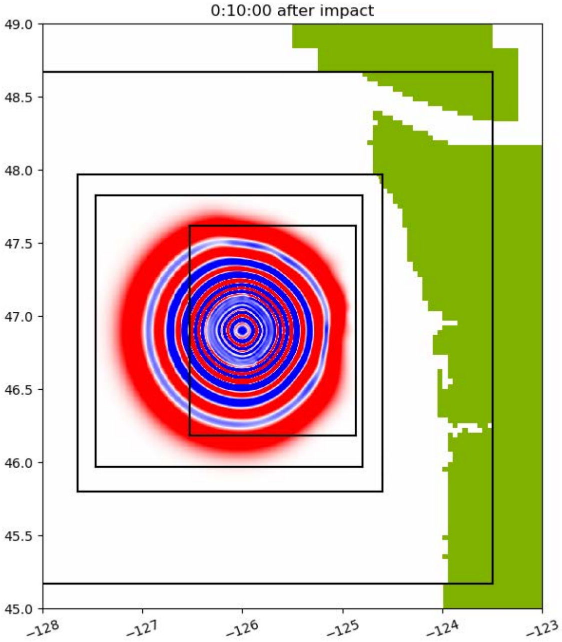
0:10:00 after impact
49.0
48.5
48.0
47.5
47.0
46.5
46.0
45.5
45.0
−128
−127
−126
−125
−124
−123

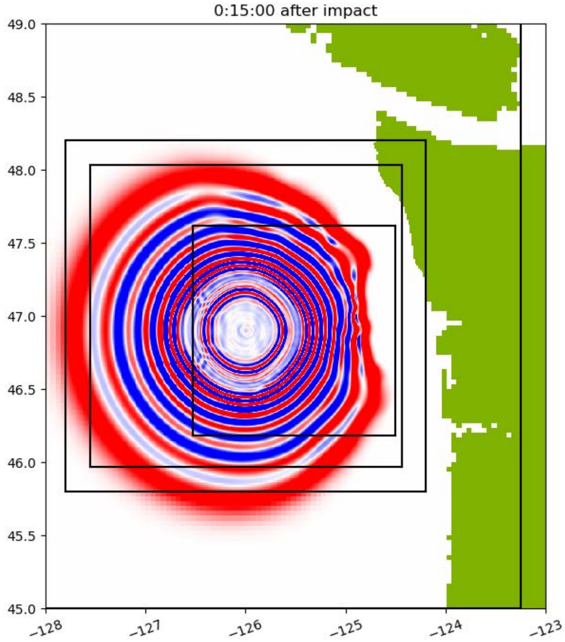
0:15:00 after impact
49.0
48.5
48.0
47.5
47.0
46.5
46.0
45.5
45.0
−128
−127
−126
−125
−124
−123

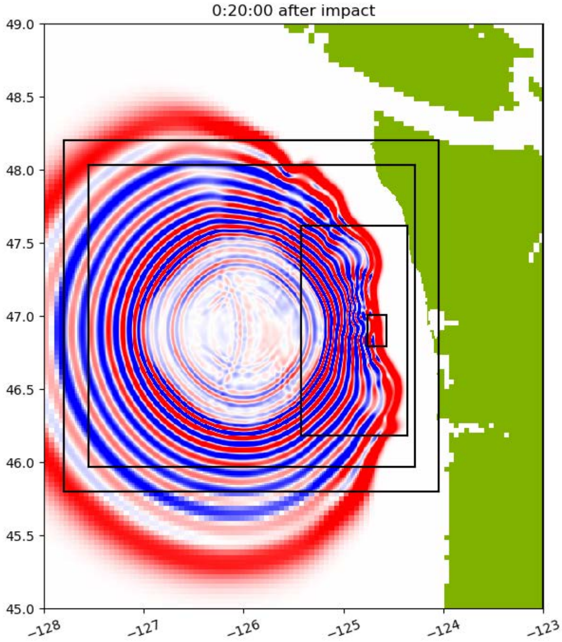
0:20:00 after impact
49.0
48.5
48.0
47.5
47.0
46.5
46.0
45.5
45.0
−128
−127
−126
−125
−124
−123

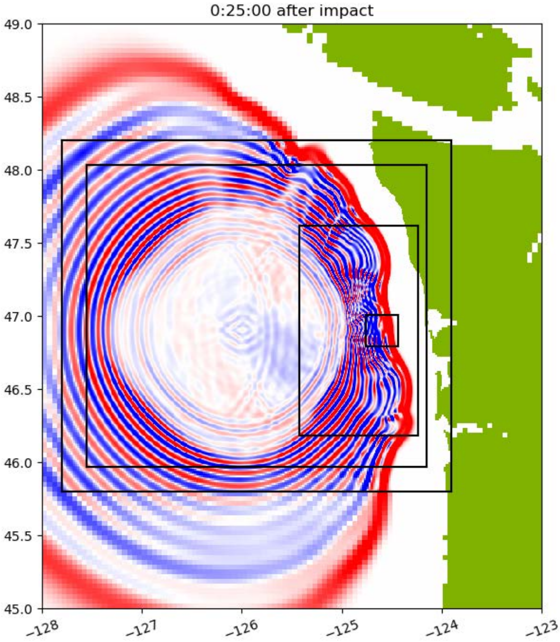
0:25:00 after impact
49.0
48.5
48.0
47.5
47.0
46.5
46.0
45.5
45.0
−128
−127
−126
−125
−124
−123

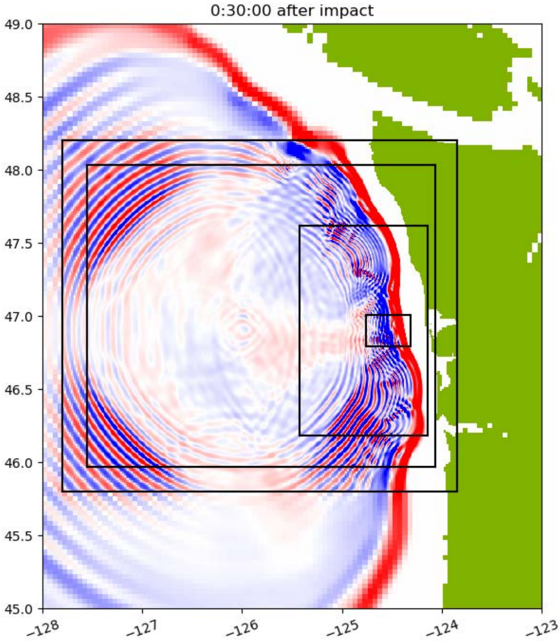
0:30:00 after impact
49.0
48.5
48.0
47.5
47.0
46.5
46.0
45.5
45.0
−128
−127
−126
−125
−124
−123

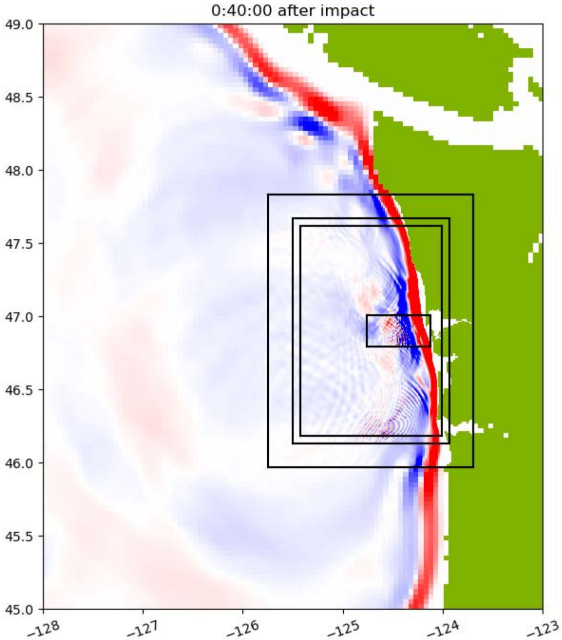
0:40:00 after impact
49.0
48.5
48.0
47.5
47.0
46.5
46.0
45.5
45.0
−128
−127
−126
−125
−124
−123

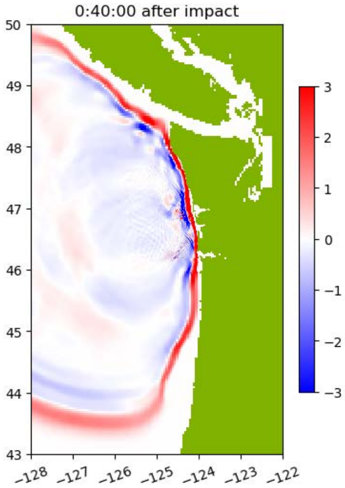

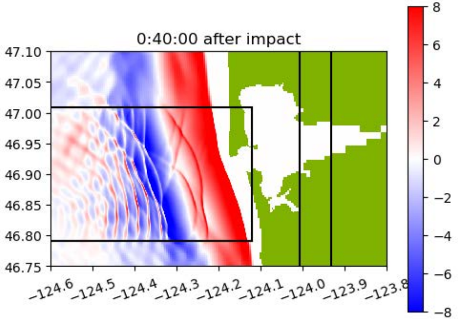

Dispersion leads to
“soliton fission” near coast.

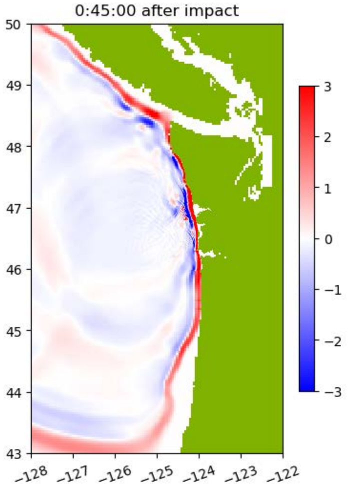

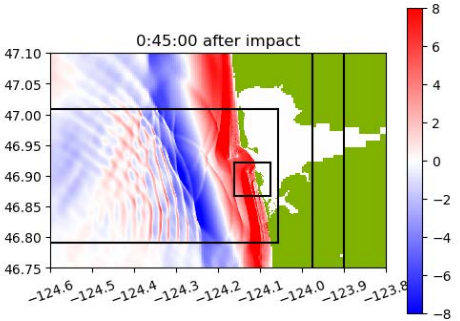

Dispersion leads to
“soliton fission” near coast.

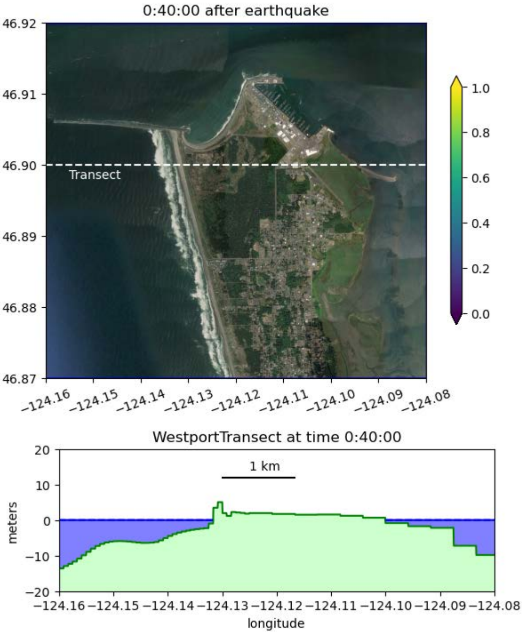
0:40:00 after earthquake
Transect
46.92
46.91
46.90
46.89
46.88
46.87
−124.16 −124.15 −124.14 −124.13 −124.12 −124.11 −124.10 −124.09 −124.08
1.0
0.8
0.6
0.4
0.2
0.0
WestportTransect at time 0:40:00
1 km
meters
20
10
0
−10
−20
−124.16 −124.15 −124.14 −124.13 −124.12 −124.11 −124.10 −124.09 −124.08
longitude

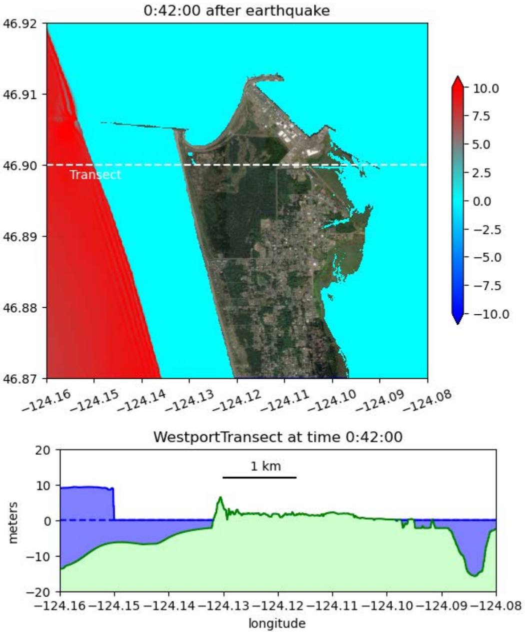
0:42:00 after earthquake
Transect
46.92
46.91
46.90
46.89
46.88
46.87
−124.16
−124.15
−124.14
−124.13
−124.12
−124.11
−124.10
−124.09
−124.08
10.0
7.5
5.0
2.5
0.0
−2.5
−5.0
−7.5
−10.0
WestportTransect at time 0:42:00
1 km
meters
20
10
0
−10
−20
longitude

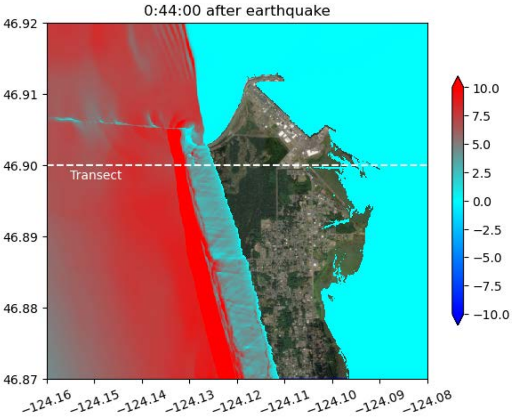

0:44:00 after earthquake
46.92
46.91
46.90
46.89
46.88
46.87
Transect
−124.16
−124.15
−124.14
−124.13
−124.12
−124.11
−124.10
−124.09
−124.08
10.0
7.5
5.0
2.5
0.0
−2.5
−5.0
−7.5
−10.0

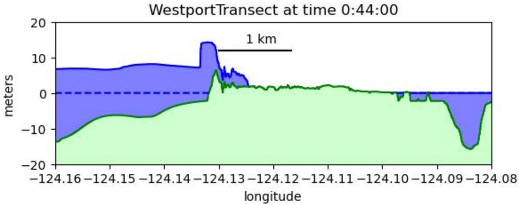

WestportTransect at time 0:44:00
1 km
meters
20
10
0
−10
−20
−124.16 −124.15 −124.14 −124.13 −124.12 −124.11 −124.10 −124.09 −124.08
longitude

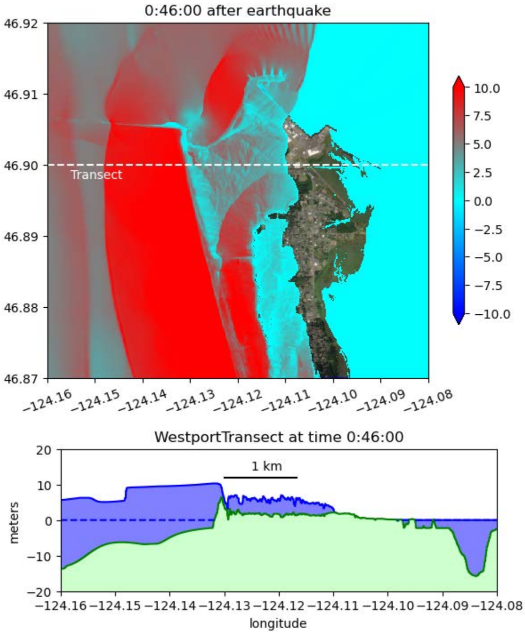
0:46:00 after earthquake
46.92
46.91
46.90
46.89
46.88
46.87
Transect
−124.16
−124.15
−124.14
−124.13
−124.12
−124.11
−124.10
−124.09
−124.08
10.0
7.5
5.0
2.5
0.0
−2.5
−5.0
−7.5
−10.0
WestportTransect at time 0:46:00
1 km
20
10
0
−10
−20
meters
longitude

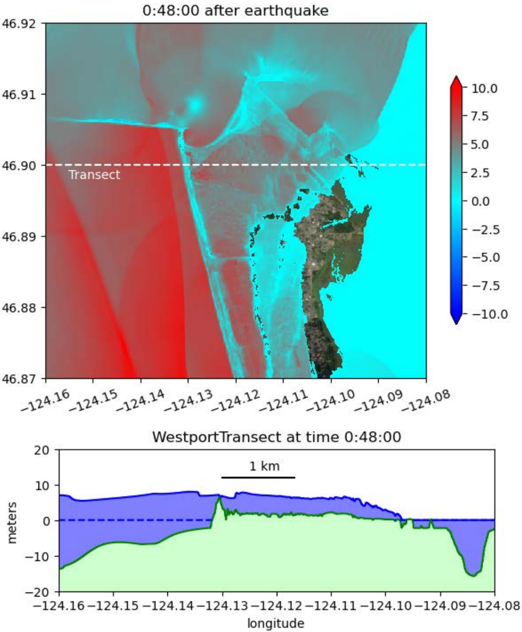
0:48:00 after earthquake
46.92
46.91
46.90
46.89
46.88
46.87
Transect
−124.16
−124.15
−124.14
−124.13
−124.12
−124.11
−124.10
−124.09
−124.08
10.0
7.5
5.0
2.5
0.0
−2.5
−5.0
−7.5
−10.0
WestportTransect at time 0:48:00
1 km
20
10
0
−10
−20
meters
longitude

Fractional step method

$$\begin{aligned} h_t + (hu)_x &= 0 \\ (hu)_t + \left(hu^2\right)_x + gh\eta_x &= \psi \end{aligned}$$

1. Solve elliptic equation for source term ψ:

$$[I - D_{11}]\psi = -D_{11}\left[\left(hu^2\right)_x + gh\eta_x\right] + gh_0^2 B_1 (h_0\eta_x)_{xx}.$$

$\Longrightarrow$ Difficulties for AMR algorithms.

2. Update momentum by $(hu)_t = \psi$ over time step
3. Take step with homogeneous SWE.

Patch-Based Adaptive Mesh Refinement

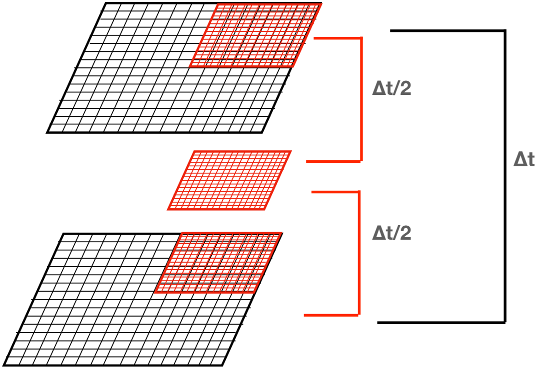

Ghost cells on border of level 2 (red grids) interpolated in space and time from level 1 (black grids), including extra variable ψ.

Conclusions and Future Work

Demonstrated: proof of concept using both Boussinesq and Shallow Water model combined with AMR.

But: cannot yet tell how much difference it makes for shoreline inundation; earlier 1D parameter studies showed significant differences

- How much does it depend on switching criteria?
  Currently switching at 10 meter depth
  Have not included “wave breaking” criteria yet
- Make more robust
  Some stability problems at patch edges
- Compare with other Bouss models
  ForestClaw + Serre-Green-Naghdi

IAA-PDC-21-09-15 ASTEROID IMPACTS - DOWNWIND AND DOWNSTREAM EFFECTS

Mount Pinatubo in the Philippines
Credit: Dave Harlow, U.S.G.S.

Timothy N. Titus, Darrel Robertson, Joel Sankey, and Larry Mastin

Tunguska Event. Credit: Getty Images

Temescal Valley, CA. Credit: abc7.com

Phoenix, AZ Haboob. Credit: Andrew Pielage

U.S. Department of the Interior
U.S. Geological Survey

Motivation

Lots of effort into initial effects!

- air blast with overpressure shock
- thermal radiation
- crater formation and ejecta deposition
- seismic shaking
- tsunamis

Are there other effects as a result of these initial effects?

- displaced in distance
- displaced in time

Down wind effects

- How far is debris blown down wind?
- Does that debris pose a threat?
- How do you characterize that threat?

Down stream effects

- How much debris will end up in the watershed?
- Is the water shed interconnected to other watersheds?
- Does that debris pose a threat to the water supply?

USGS science for a changing world

Motivation

At what size of impactor do downstream and downwind effects matter?

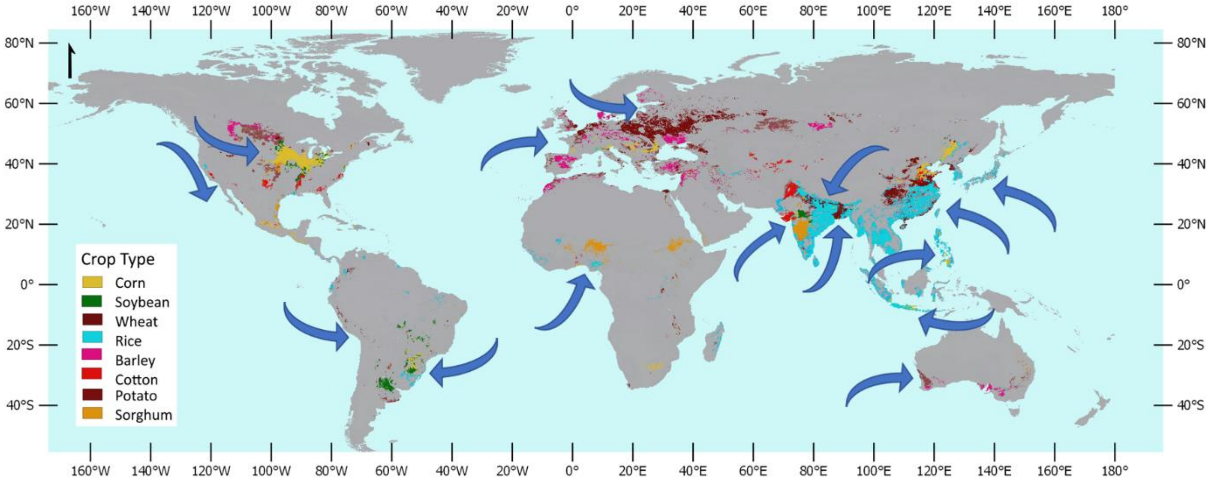

Data sources: Crop data from Sacks et al. 2010. Wind data from IRI 2020, accessed 5/20/2020.
Credit: Adam Oliphant.

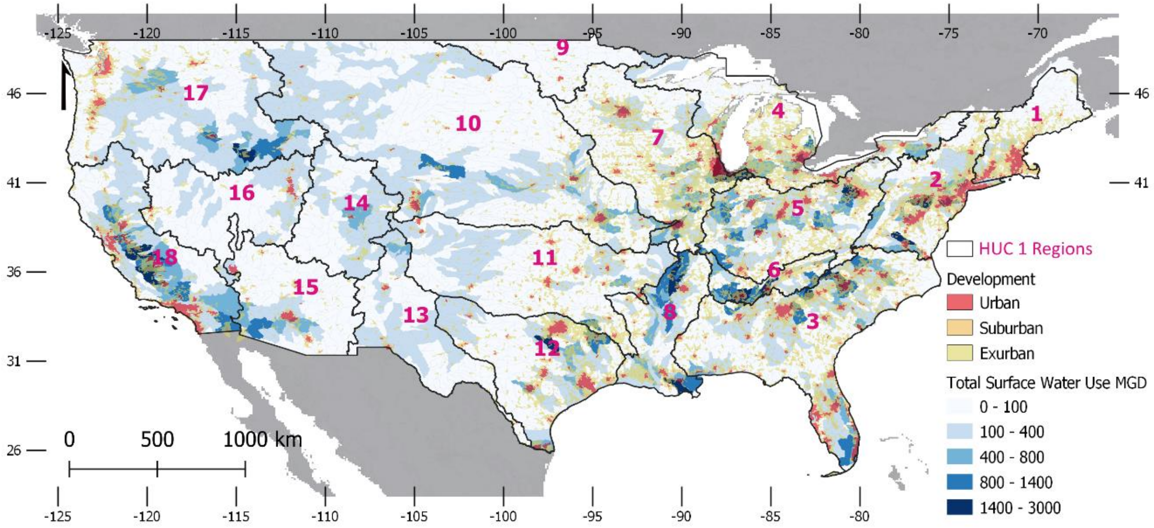

Data sources: HUC watersheds boundaries from Watershed Boundary Dataset (USDA 2019, Accessed September 1, 2009.),

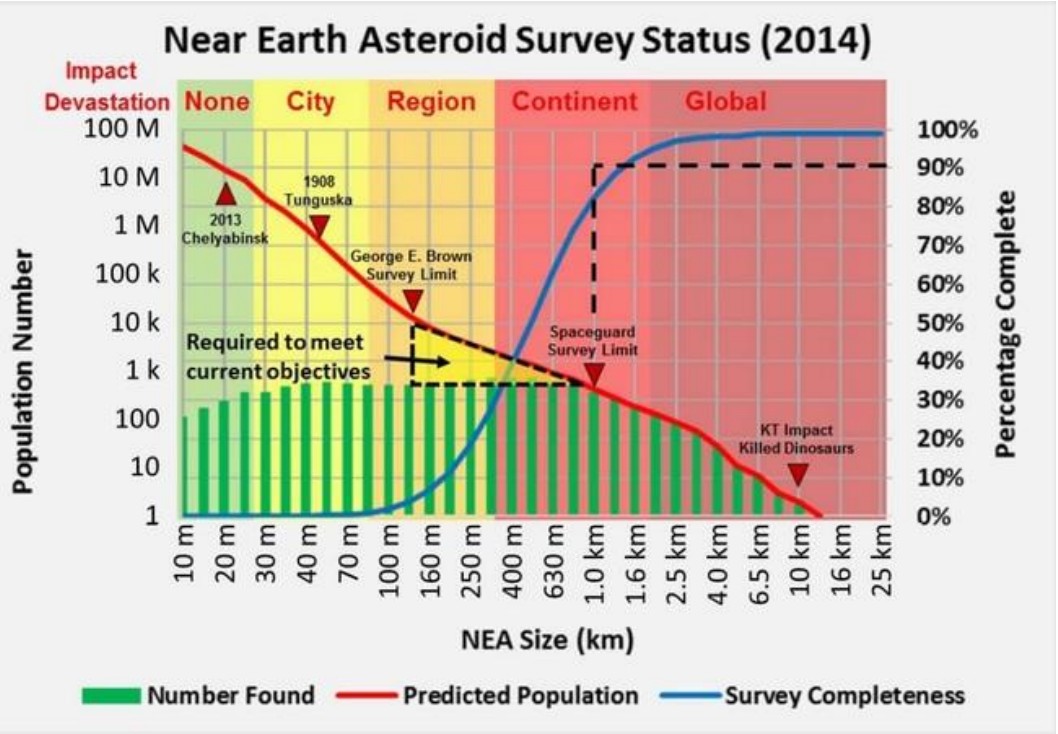

Credit: White House

USGS science for a changing world

Characterization using more common hazards

Downwind

- **Volcanic eruptions**
- Dust storms
- Wildfires

Downstream

- **Wildfires**
- Landslides
- Floods

Tunguska Event. Credit: Getty Images

Near Williams Lake, B.C. Credit: © PC/DARRYL DYCK

Mount Pinatubo. Credit: Dave Harlow, U.S.G.S.

Phoenix, AZ Haboob. Credit: Andrew Pielage

Temescal Valley, CA. Credit: abc7.com

Impact scenario:

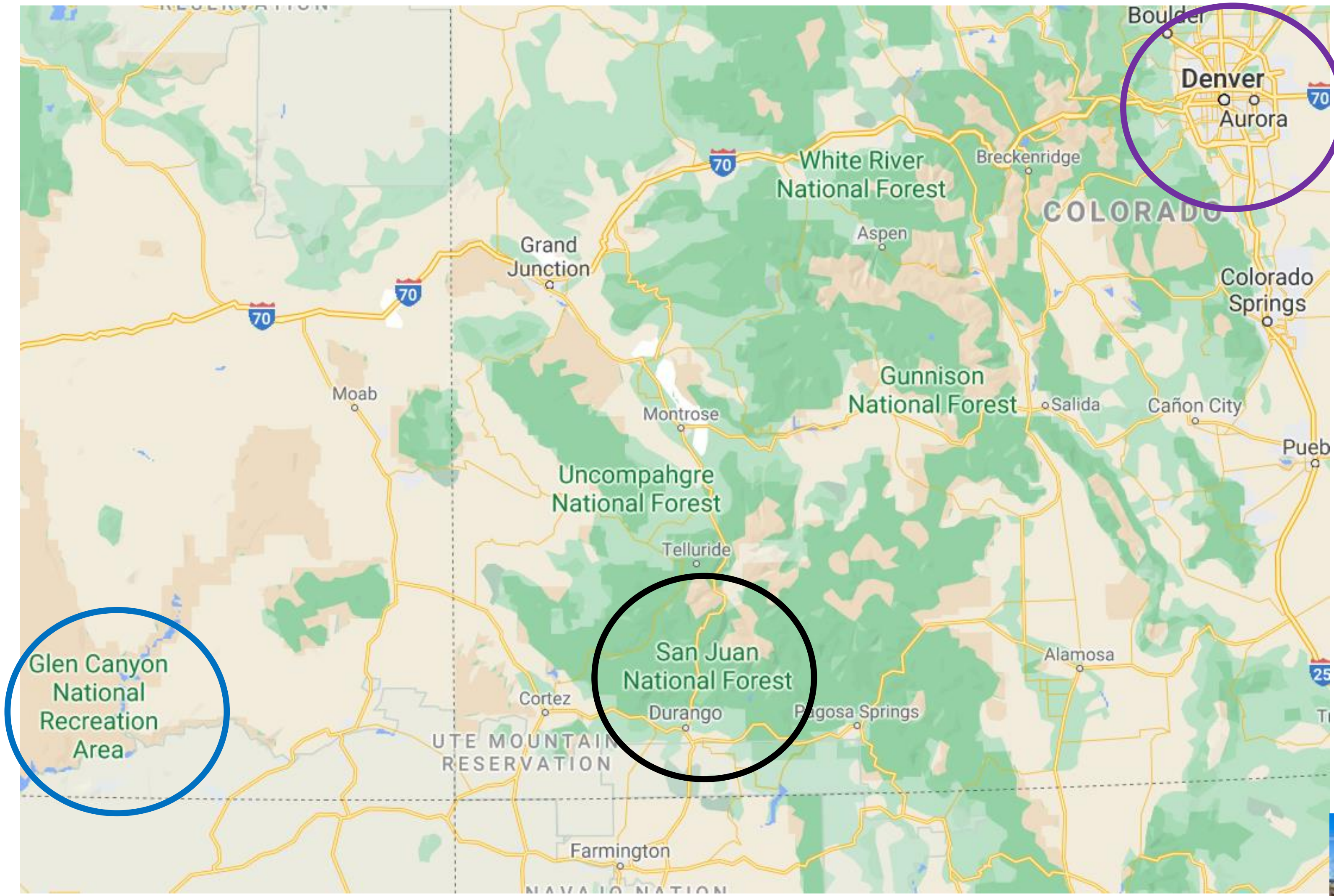

Credit: Google Maps

San Juan Mountains, in southwestern Colorado :

- Low population
- Headwaters of the Colorado River
- Upwind from Agriculture and Transportation hubs and corridors.

A 120-meter impactor is the median expected size. We chose impactor sizes ranging from 42-meters to 600-meters

Tunguska Event.. Credit: Getty Images

Meteor Crater, AZ Credit: CC BY-SA 4.0

USGS science for a changing world

Downwind

- USGS Ash3D
    - Date/Time → Wind Patterns
    - Mass of the impactor deposited at 40 km AGL.
- → Downwind distribution

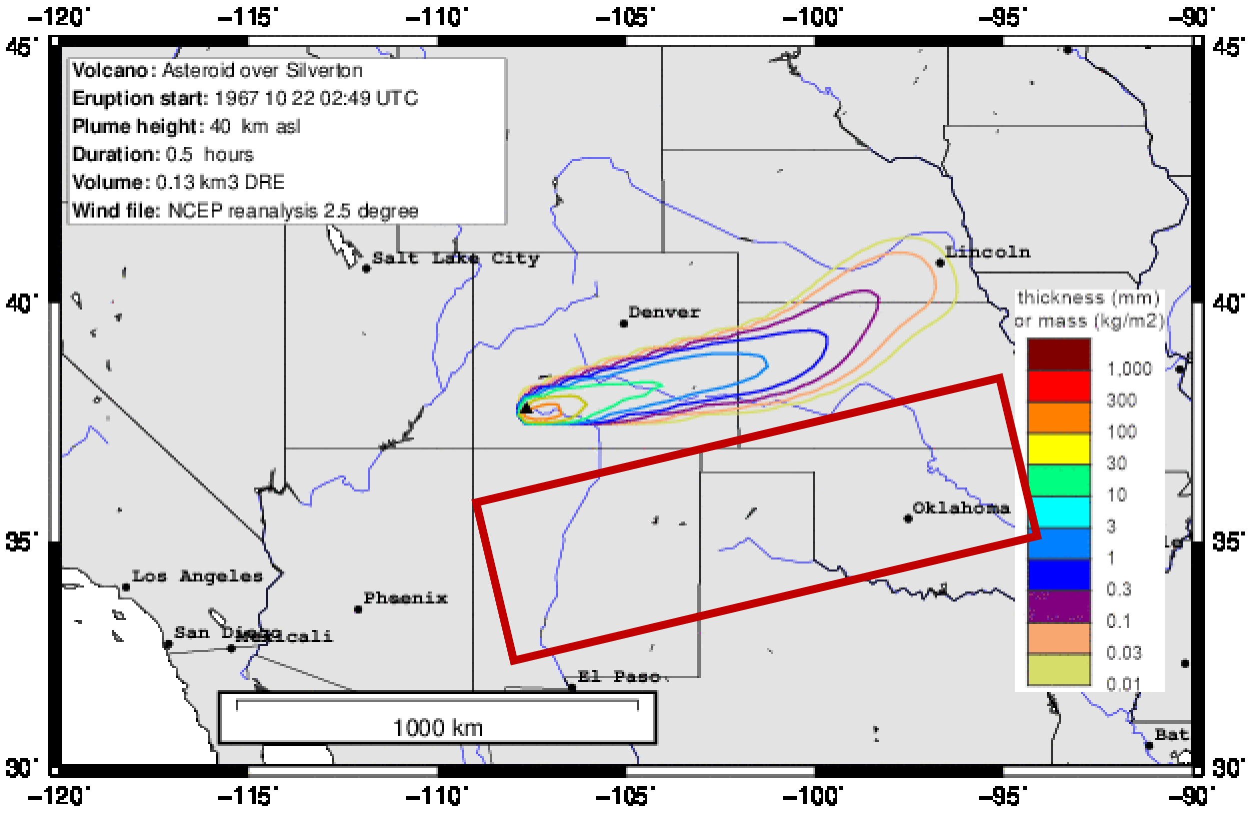

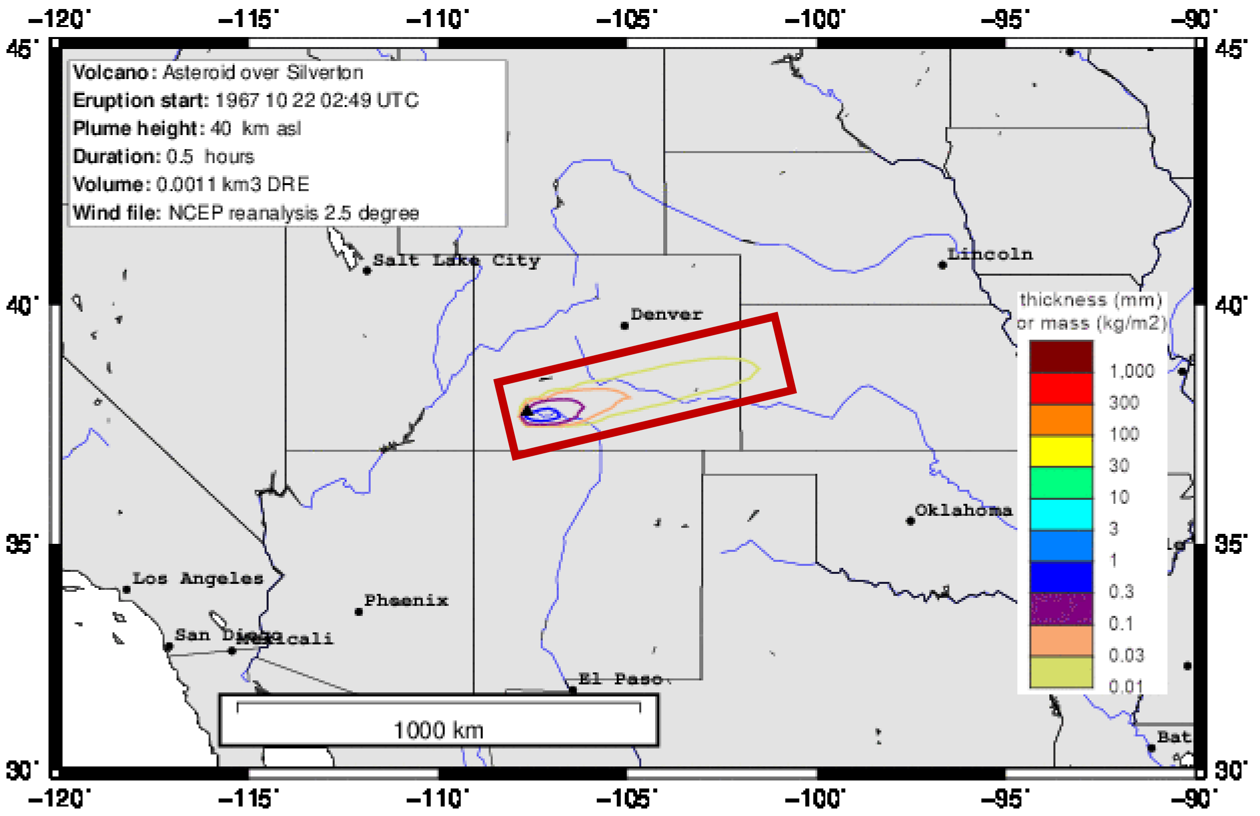

- Results for Oct 22 (1967):
    - Above – 120-m Impactor
    - Lower Left – 600-m Impactor
    - The lowest contour is 10 um of dust/ash/debris.
    - Within hours, will affect air quality and transportation corridors.

USGS
science for a changing world

Downstream

Diameter (m)	Radius of Ignition (km)	Burn Area (km2)	Burn Area (ha)	Sankey et al. (2017) Annual Post-fire Sediment Yields (Mg/ha)	Watershed Sediment Yield from Post Impact Soil Erosion (Mg)
42	3.90	47.78	4,778.22	0.83	3,966
65	6.50	132.73	13,272.84	0.83	11,016
120	13.40	564.09	56,408.77	0.83	46,819
350	47.20	6,998.76	699,875.94	0.83	580,897
600	89.20	24,995.78	2,499,578.46	0.83	2,074,650
42	3.90	47.78	4,778.22	6.76	32,301
65	6.50	132.73	13,272.84	6.76	89,724
120	13.40	564.09	56,408.77	6.76	381,323
350	47.20	6,998.76	699,875.94	6.76	4,731,161
600	89.20	24,995.78	2,499,578.46	6.76	16,897,150
42	3.90	47.78	4,778.22	60.80	290,516
65	6.50	132.73	13,272.84	60.80	806,989
120	13.40	564.09	56,408.77	60.80	3,429,653
350	47.20	6,998.76	699,875.94	60.80	42,552,457
600	89.20	24,995.78	2,499,578.46	60.80	151,974,370

- Impactor size → debris area
- Debris area + Yield rate → annual yield
  - Yield rate is determined from modeled erosion rates
  - Does not include effect of blast generated debris
- Annual yield / normal annual yield → Increase in annual sediment yield
- Current Annual Yield → 1.83×10^7 Mg/yr
- Comparison
  - 350m: x 2.3
  - 600m: x 8.3

USGS science for a changing world

Summary

Downwind

- 120-m impactor will have effects on
  - Southern Colorado
  - Air quality (Human/Livestock)
  - Ground Visibility (e.g I-25)
  - Air Corridors
- 600-m impactor
  - Colorado, Nebraska, Kansas
  - Air quality
  - Ground Visibility
  - Air Hubs & Corridors

Downstream

- 350-m/600-m impactors will have effects
  - Southern Colorado/Northern New Mexico
  - Flooding potential
  - Water Quality (turbidity, toxicity)
- Minimal impact of Glen Canyon Dam operations
- Our sediment yields are likely conservative

ROYAL OBSERVATORY OF BELGIUM

UNITED NATIONS
Office for Outer Space Affairs

7th IAA Planetary Defense Conference

26-30 April 2021, Online Event

Hosted by UNOOSA in collaboration with ESA

Environmental Consequences of asteroid impacts by General Circulation Model (GCM) simulations

Cem Berk Senel[1,*], Orkun Temel[1,2], and Ozgur Karatekin[1]

[1] Reference Systems and Planetology Department, Royal Observatory of Belgium, Belgium

[2] KU Leuven, Institute of Astronomy, Leuven, Belgium

[*] Corresponding author, email: **cem.berk@observatory.be**

1- Motivation & Methodology

asteroidImpactWRF: to simulate the climatic response of small and large impactors

Table 1:

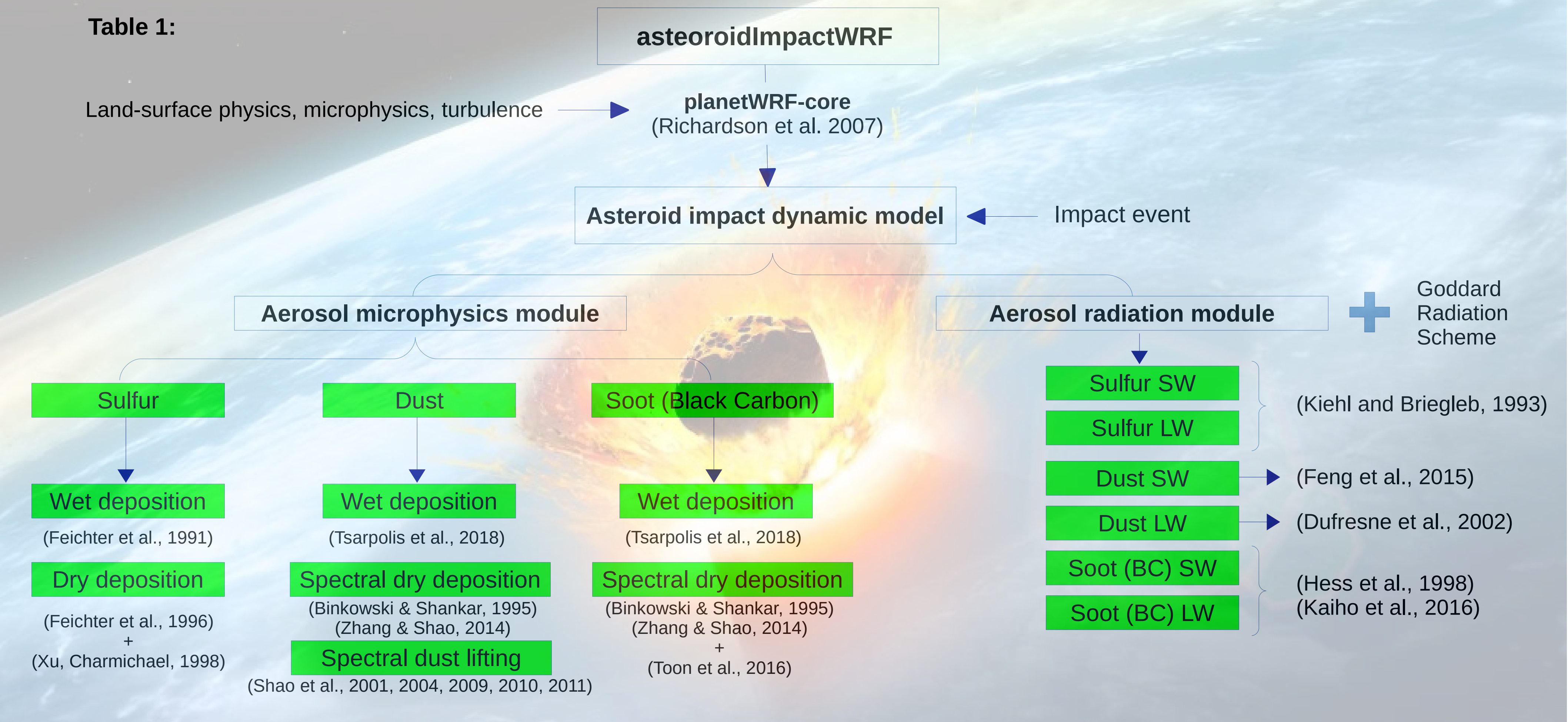

1- Methodology
General Circulation Model (GCM) set-up

GCM set-up

- The horizontal grid spacing is 5° through the zonal and meridional directions, having 21 vertical eta layers.
- Goddard radiation model [Chou and Suarez, 1999, Chou et al., 2001] is used for the shorthwave and longwave radiative transfer.
- The aerosol (dust, sulfur, soot) microphysics (lifting, dry/wet deposition) and radiation is modeled as given in Table 1.
- Boundary-layer turbulence is modeled by the Bougeault–Lacarrere Scheme (BouLac) [Bougeault and Lacarrere, 1989].
- For the parameterization of microphysical processes, double-moment 6–class microphysics scheme is used [Lim and Hong, 2010].
- 5–layer thermal diffusion scheme is utilized for land-surface physics [Dudhia, 1996], the surface layer is modeled by the revised MM5 scheme [Jiménez et al., 2012].
- For the ocean model, one-dimensional ocean mixed layer model (OMLM) is used [Pollard et al., 1973].

Aerosol injection scenarios -based on Toon et al. (1997, 2016)-

Description of GCM experiments: Impact scenarios

- In the current study, we perform 2 impact scenarios based on 2 different aerosol types (dust and sulfur), depending on 3 different impactor sizes (i.e. diameter) ranging between:
  - 100 m (similar to hypothetical PDC2019 impactor)
  - 1 km
  - 10 km (corresponding to a similar size of Chicxulub impactor)
- The center location of impact event is set to be New York city (∼ 40.7°N, 74.0°W), based upon the hypothetical asteroid impact scenario from PDC2019.
- GCM simulations are performed for the present Earth's climate conditions taking the globally-averaged atmospheric CO_2 concentration to be nearly 416 parts per million (ppm).
- Time integration for each simulation is carried out for 5 years where the first 3-years are removed out (initial spin-up).

GCM Experiment	Impactor Dia. $[km]$	Impact Energy $[Mt]$	Injected Aerosol Mass $[g]$
Dust-pdc2019	0.1	68	$1.4x10^{12}$
Dust-1km	1	6800	$1.4x10^{15}$
Dust-chicxulub	10	$6.8x10^{7}$	$2.3x10^{18}$
Sulfur-pdc2019	0.1	68	$9.9x10^{10}$
Sulfur-1km	1	6800	$4.4x10^{13}$
Sulfur-chicxulub	10	$6.8x10^{7}$	$9.0x10^{16}$

2- Results: Dust injection

Diurnal surface temperature before and after impact - GCM experiment: Dust-PDC2019

EXERCISE

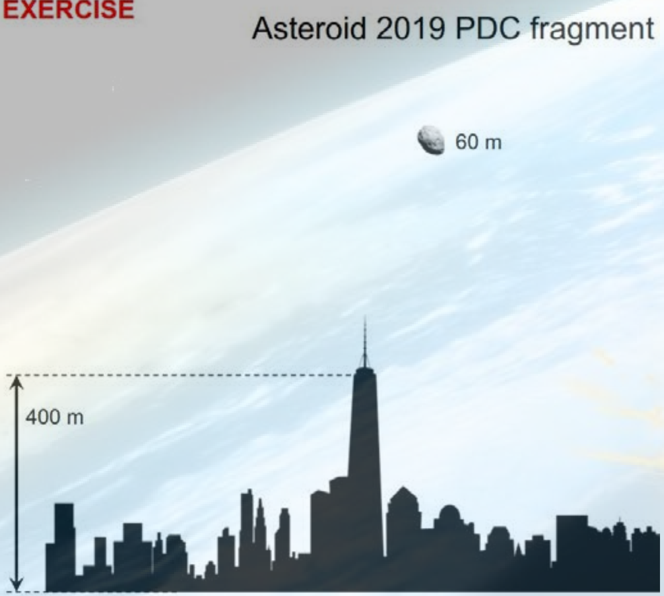

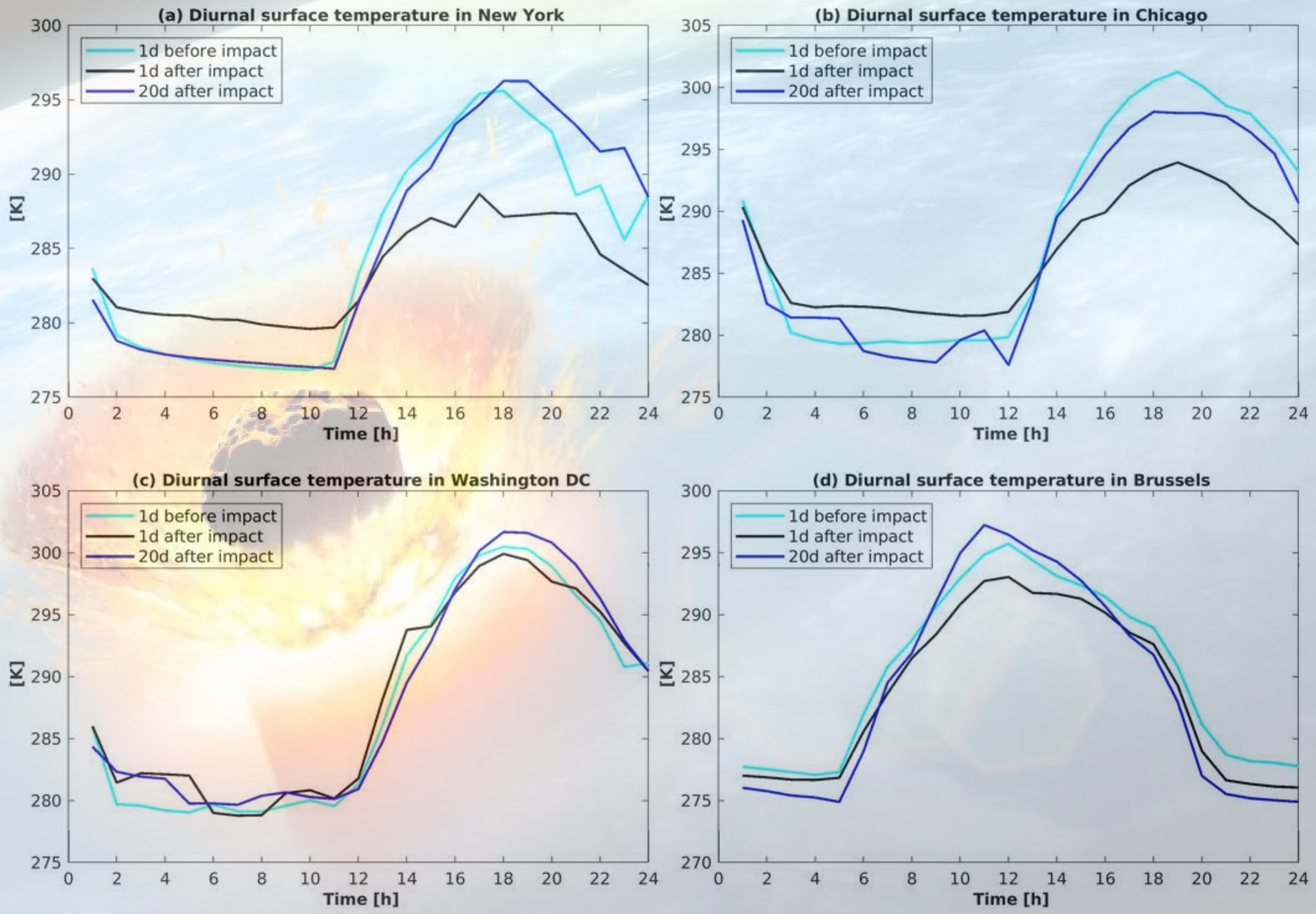

2- Results: Dust injection

Daily mean surface temperature before and after impact - GCM experiment: Dust-1km

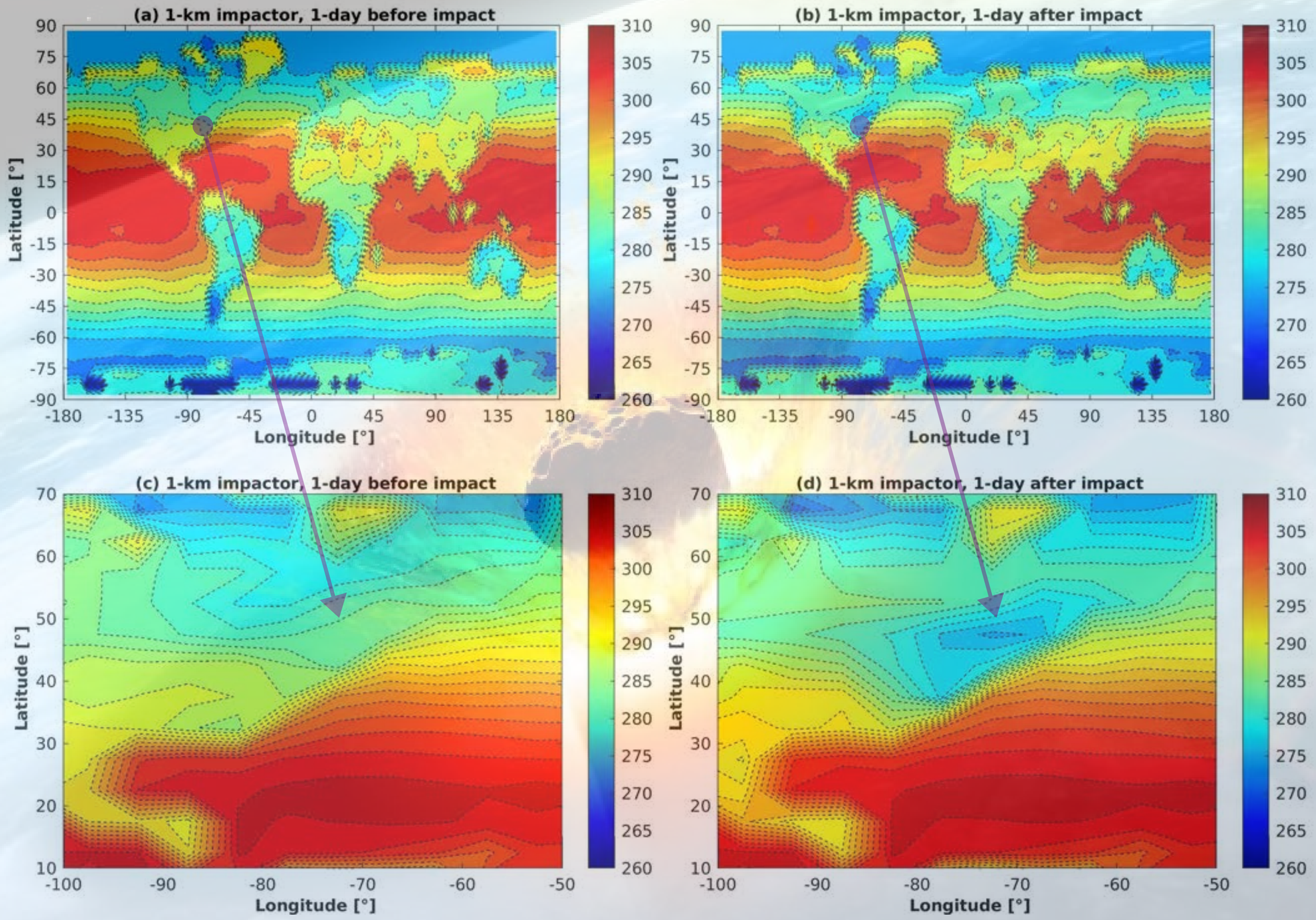

2- Results: Dust injection

Diurnal surface temperature before and after impact - GCM experiment: Dust-1km

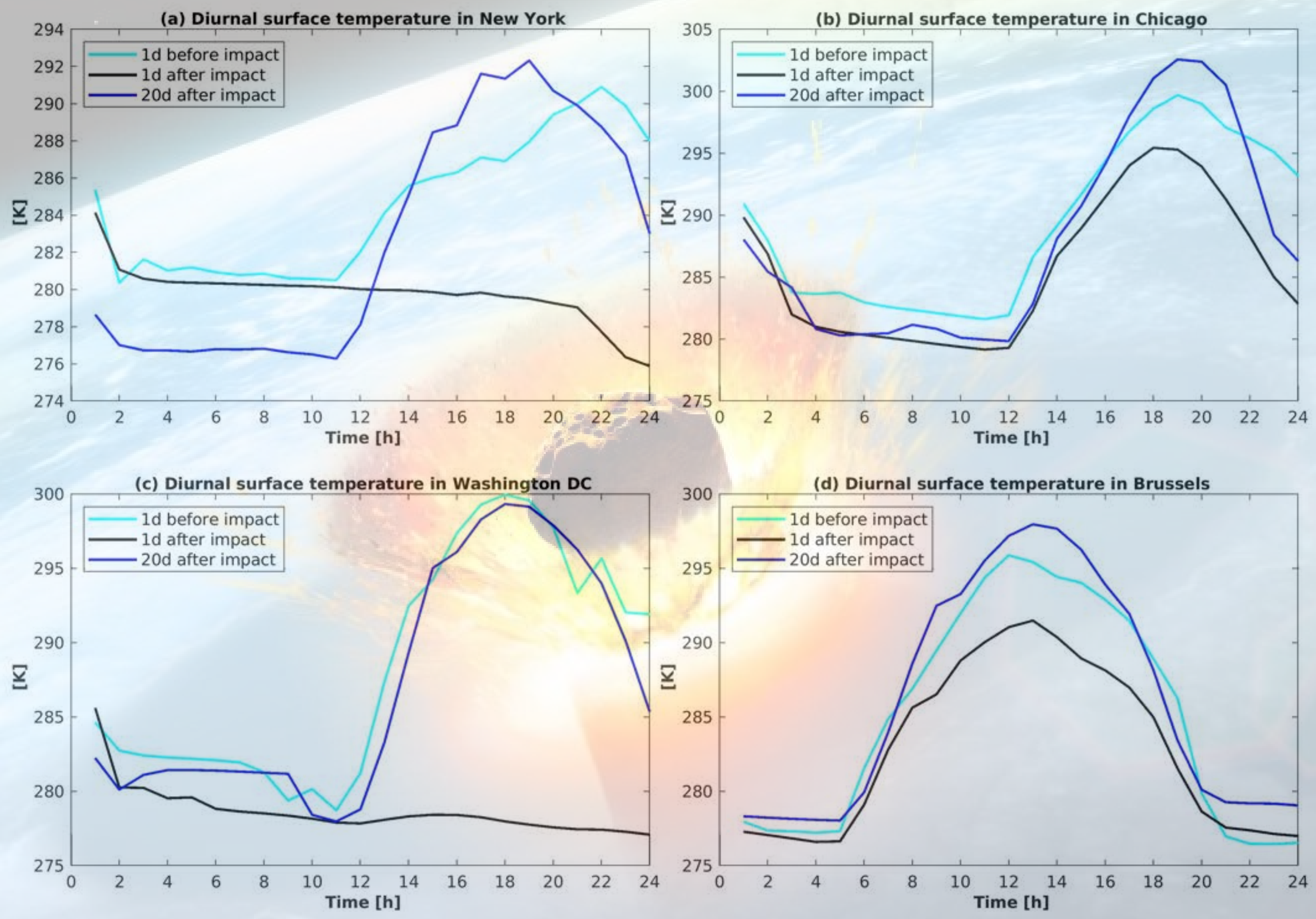

2- Results: Dust injection

Daily mean surface temperature before and after impact - GCM experiment: Dust-Chicxulub

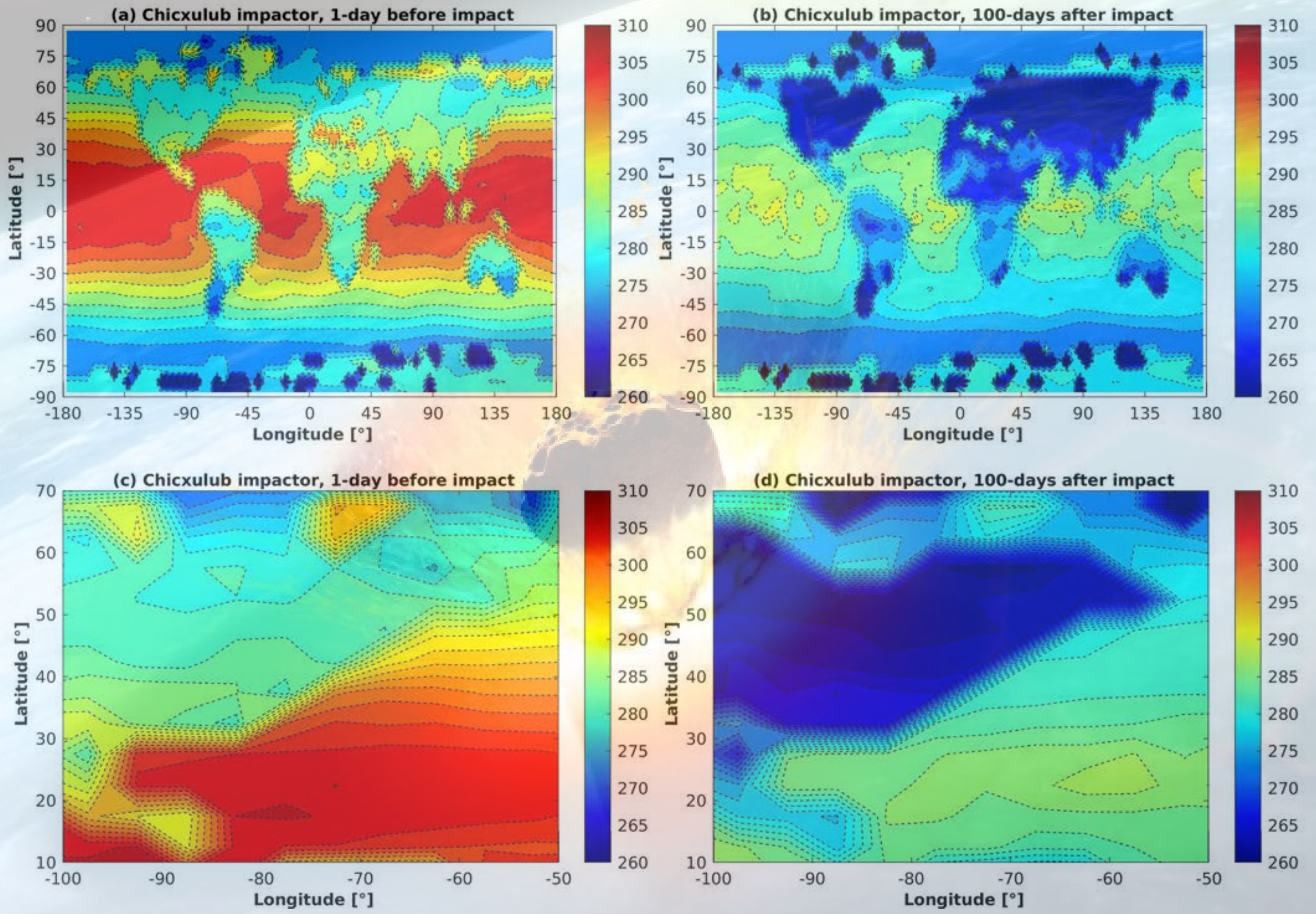

Impact Winter

3- Results: Sulfur injection

Daily mean surface temperature before and after impact - GCM experiment: Sulfur-1km

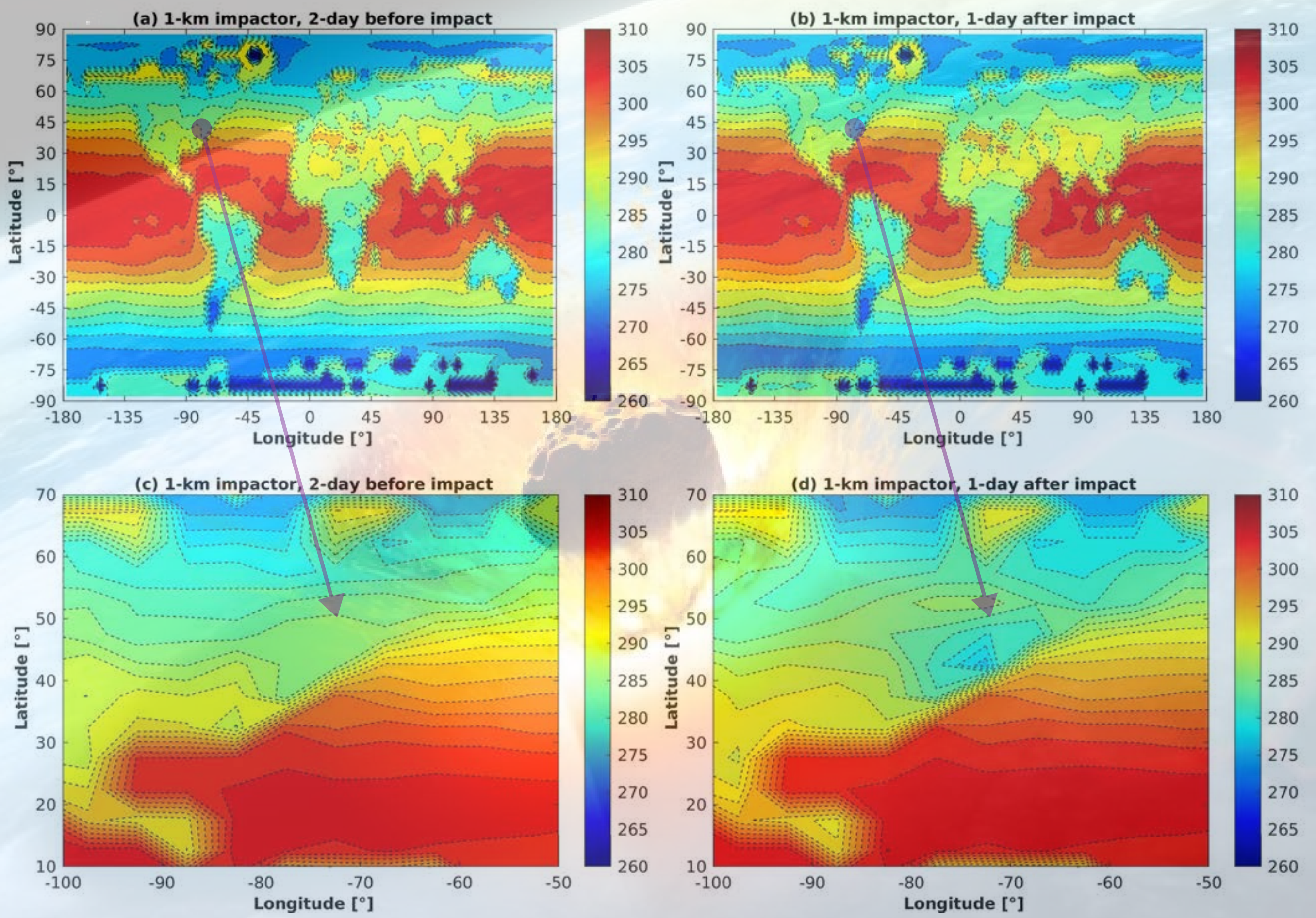

4. Next step

- **GCM grid resolution will be refined: from Δ=5°x5° to Δ=1°x1° resolutions.**
- **Aerosol microphysics and radiation will be treated via two-moment framework based on Morrison, H., & Gettelman, A. (2008).**
- **Impact-induced soot (black carbon) emission will be taken into account.**
- **Surface radiative fluxes and precipitation rates will be investigated in detail following small/large asteroid impact events.**

Thank you for your attention.

email: **cem.berk@observatory.be**

References

Toon, O. B., Zahnle, K., Morrison, D., Turco, R. P., & Covey, C. (1997). Environmental perturbations caused by the impacts of asteroids and comets. Reviews of Geophysics, 35(1), 41-78.

Toon, Owen B., Charles Bardeen, and Rolando Garcia. "Designing global climate and atmospheric chemistry simulations for 1 and 10 km diameter asteroid impacts using the properties of ejecta from the K-Pg impact." Atmospheric Chemistry and Physics 16.20 (2016): 13185-13212.

Upchurch Jr, G. R., Kiehl, J., Shields, C., Scherer, J., & Scotese, C. (2015). Latitudinal temperature gradients and high-latitude temperatures during the latest Cretaceous: Congruence of geologic data and climate models. Geology, 43(8), 683-686.

Lim, K. S. S., & Hong, S. Y. (2010). Development of an effective double-moment cloud microphysics scheme with prognostic cloud condensation nuclei (CCN) for weather and climate models. Monthly weather review, 138(5), 1587-1612.

Dudhia, J. (1996, July). A multi-layer soil temperature model for MM5. In Preprints, The Sixth PSU/NCAR mesoscale model users' workshop (pp. 22-24).

Bougeault, P., & Lacarrere, P. (1989). Parameterization of orography-induced turbulence in a mesobeta--scale model. Monthly weather review, 117(8), 1872-1890.

Shao, Y. (2001). A model for mineral dust emission. Journal of Geophysical Research: Atmospheres, 106(D17), 20239-20254.

Shao, Y. (2004). Simplification of a dust emission scheme and comparison with data. Journal of Geophysical Research: Atmospheres, 109(D10).

Shao, Y., Ishizuka, M., Mikami, M., & Leys, J. F. (2011). Parameterization of size-resolved dust emission and validation with measurements. Journal of Geophysical Research: Atmospheres, 116(D8).

Richardson, M. I., Toigo, A. D., & Newman, C. E. (2007). PlanetWRF: A general purpose, local to global numerical model for planetary atmospheric and climate dynamics. Journal of Geophysical Research: Planets, 112(E9).

Pollard, R. T., Rhines, P. B., & Thompson, R. O. (1973). The deepening of the wind-mixed layer. Geophysical Fluid Dynamics, 4(4), 381-404.

Chou, M. D., & Suarez, M. J. (1999). A solar radiation parameterization for atmospheric studies (Vol. 15, p. 38). National Aeronautics and Space Administration, Goddard Space Flight Center, Laboratory for Atmospheres, Climate and Radiation Branch.

Chou, M. D., Suarez, M. J., Liang, X. Z., Yan, M. M. H., & Cote, C. (2001). A thermal infrared radiation parameterization for atmospheric studies.

Backup: Methodology
Verification of the model at the latest Cretaceous conditions

asteroidImpactWRF

Land-surface physics, microphysics, turbulence → **planetWRF-core** (Richardson et al. 2007)

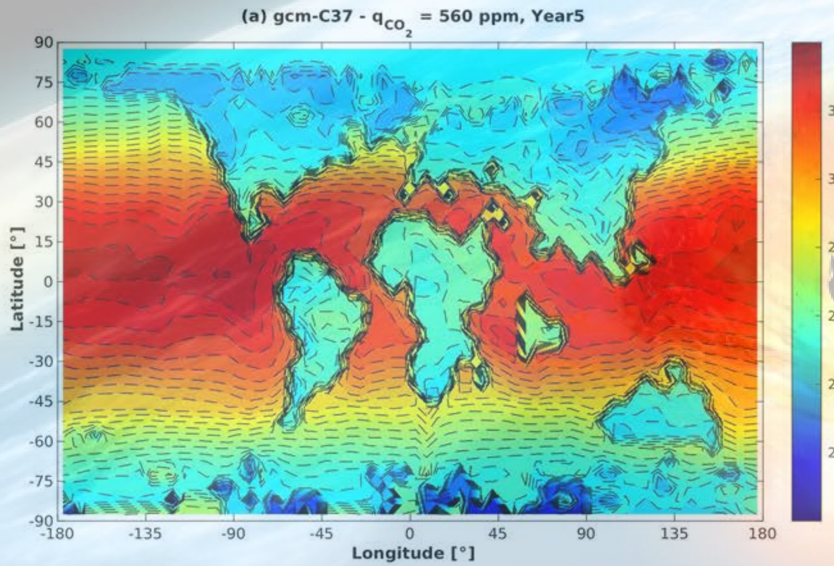

Pre-impact surface temperature [K] contours

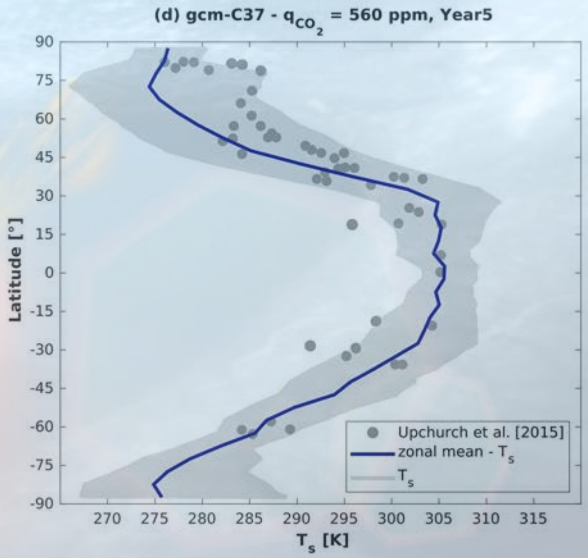

Min, max and zonally-averaged surface temperature

Upchurch et al. (2015)
Latitudinal temperature gradients and high-latitude temperatures during the latest Cretaceous: Congruence of geologic data and climate models, Geology, 43(8), 683–686

Bayesian Inference of Asteroid Physical Properties: Application to Impact Scenarios

Jessie Dotson, Lorien Wheeler,
Clemens Rumpf, & Donovan Mathias

NASA Ames Research Center

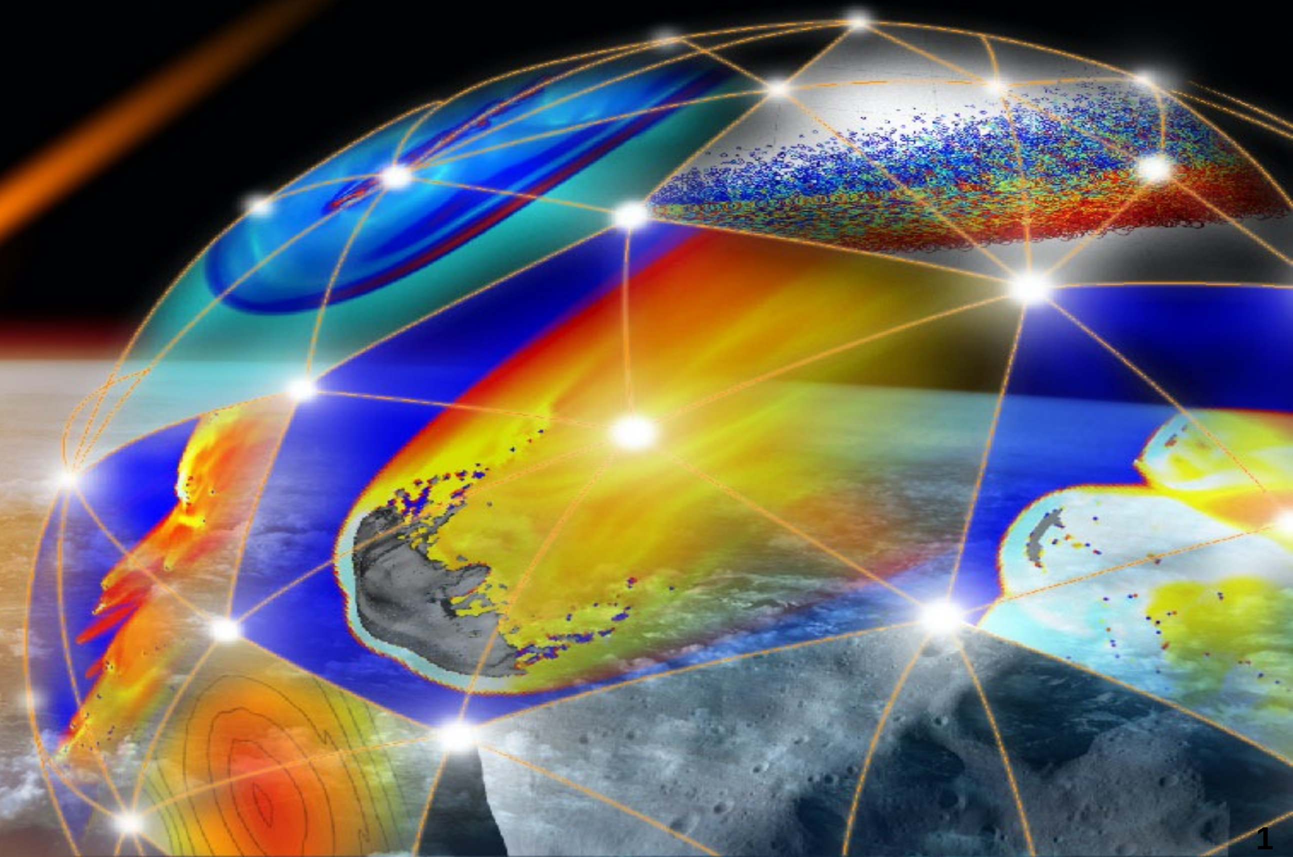

Probabilistic Asteroid Impact Risk Model

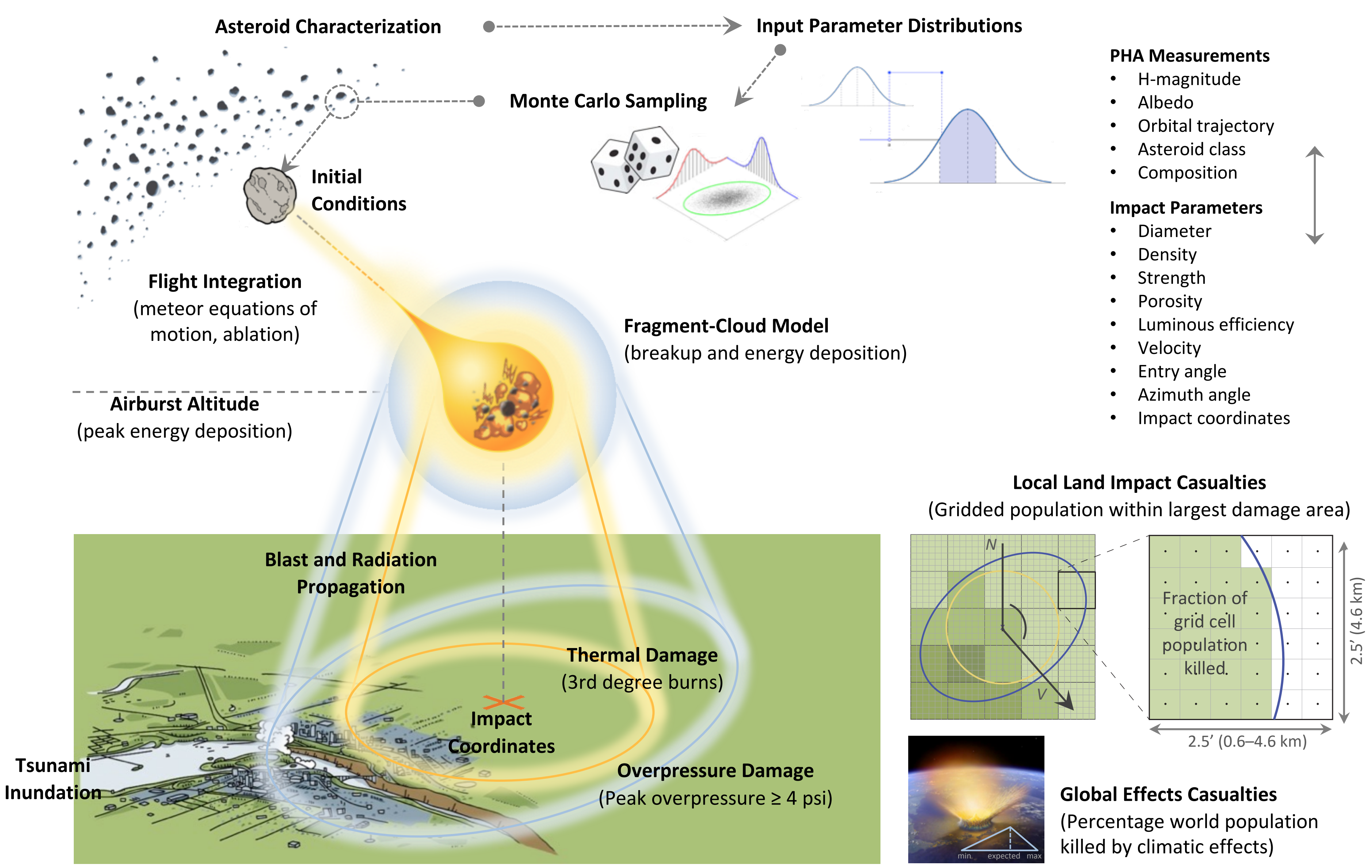

Mathias 2017

Probabilistic Asteroid Impact Risk Model

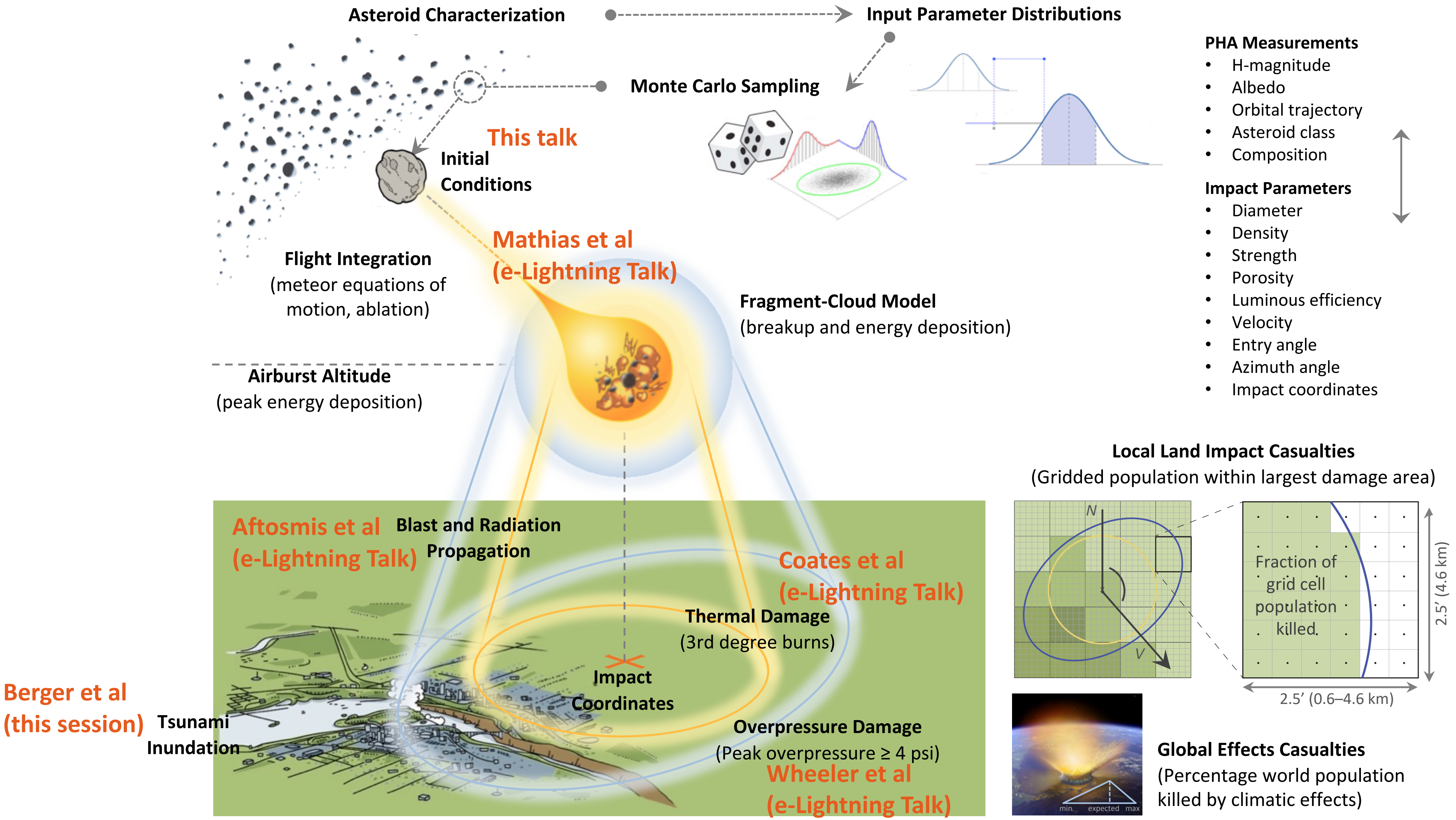

Asteroid Physical Property Risk Model Inputs

- diameter
- density
- porosity
- strength

Asteroid Physical Property Inference Network

Goal: generate virtual impactors such that

1. the distribution of values are plausible and appropriate for the scenario
2. the combination of values for any virtual impactor is physically plausible

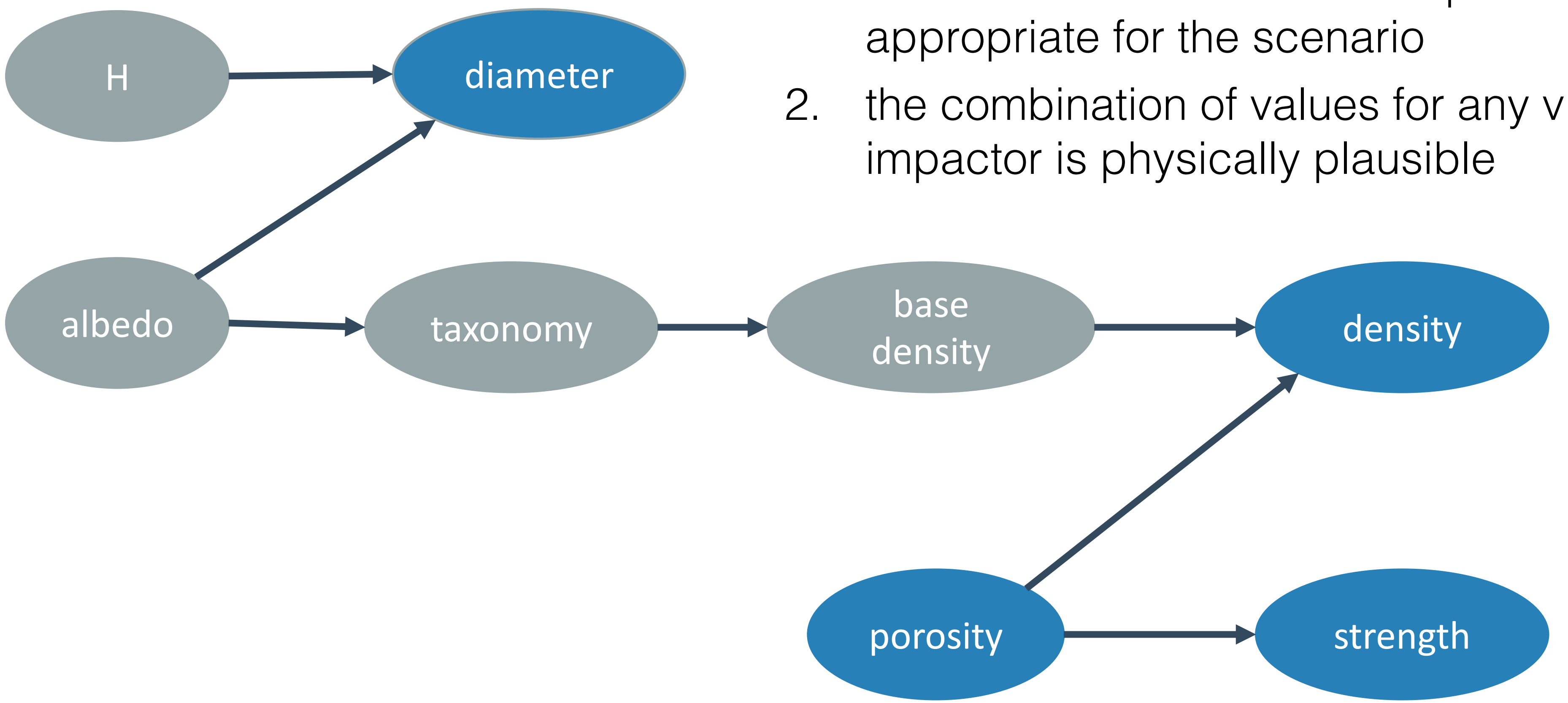

Data Derived Properties

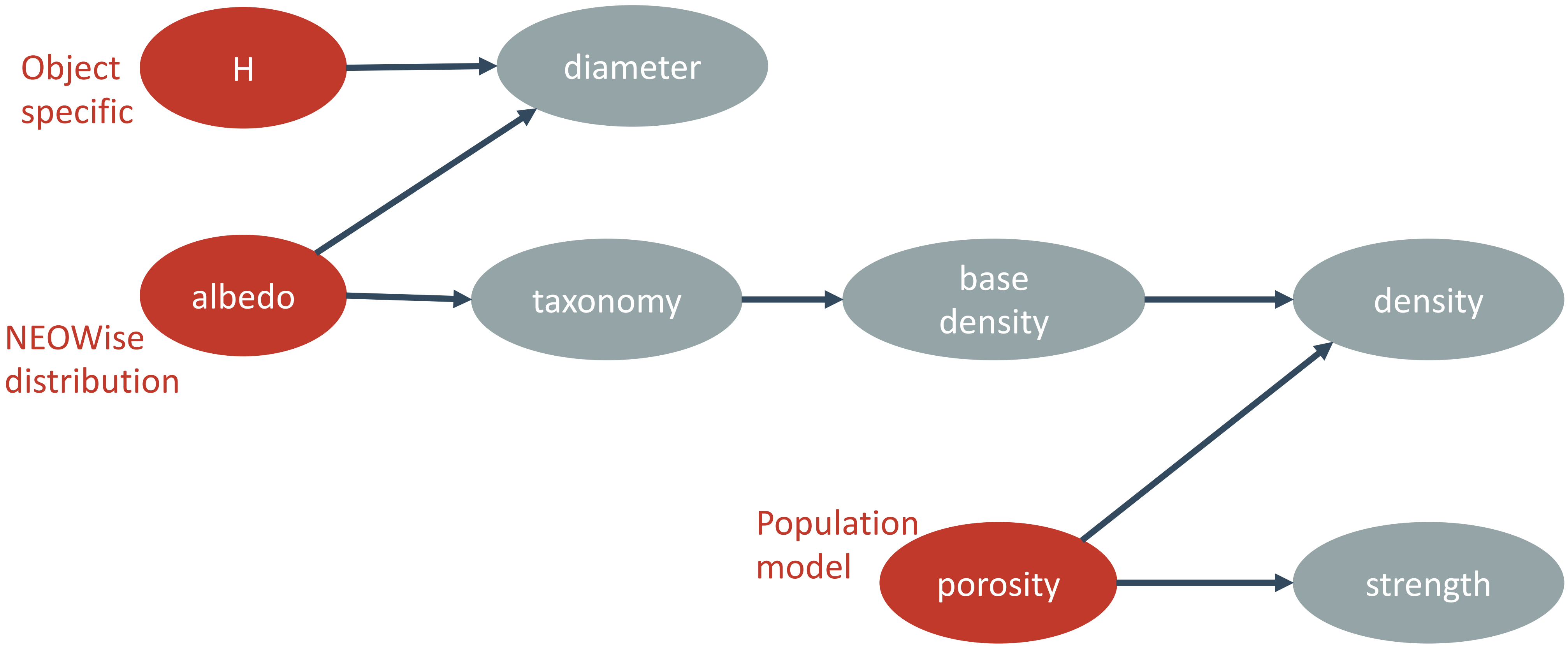

Calculated Properties

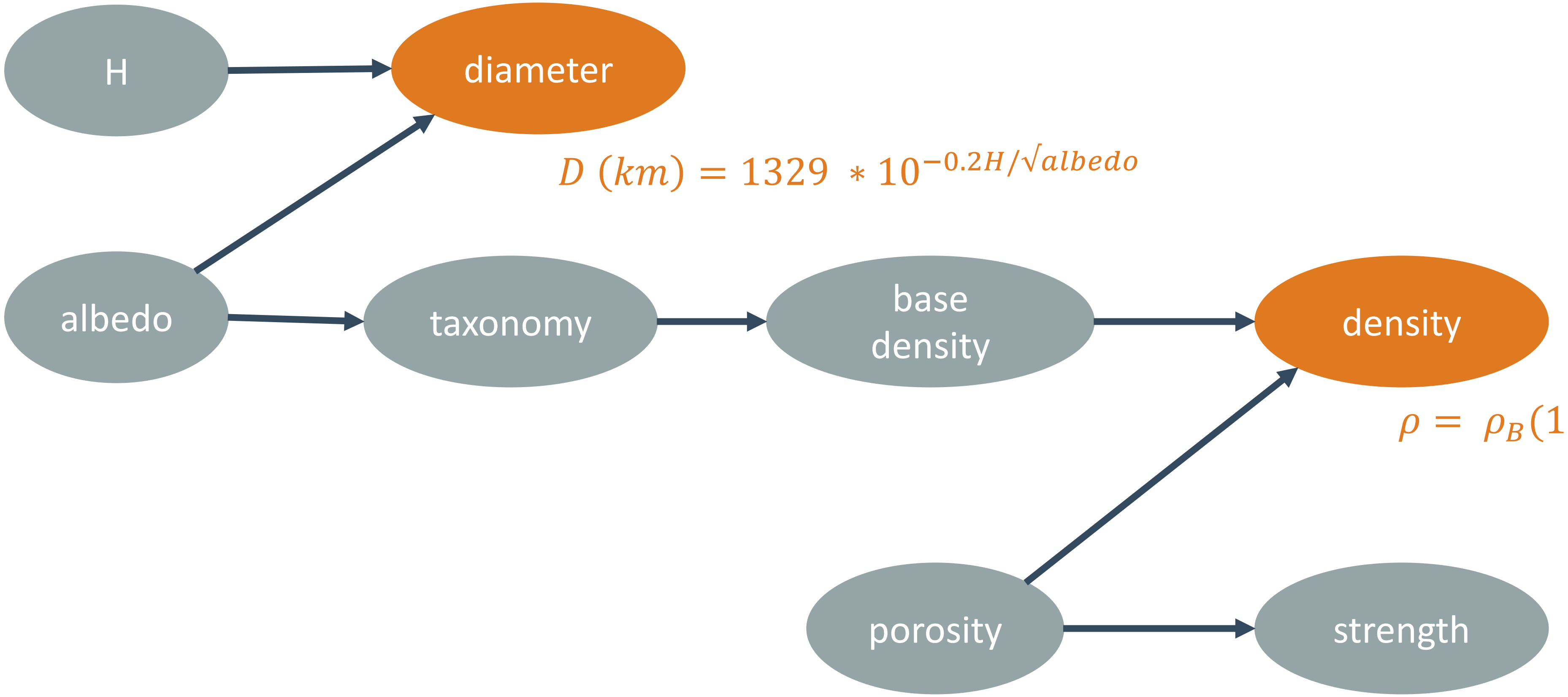

$$D\ (km) = 1329\ * 10^{-0.2H}/\sqrt{albedo}$$

$$\rho = \rho_B(1 - \text{porosity})$$

Inferred Properties

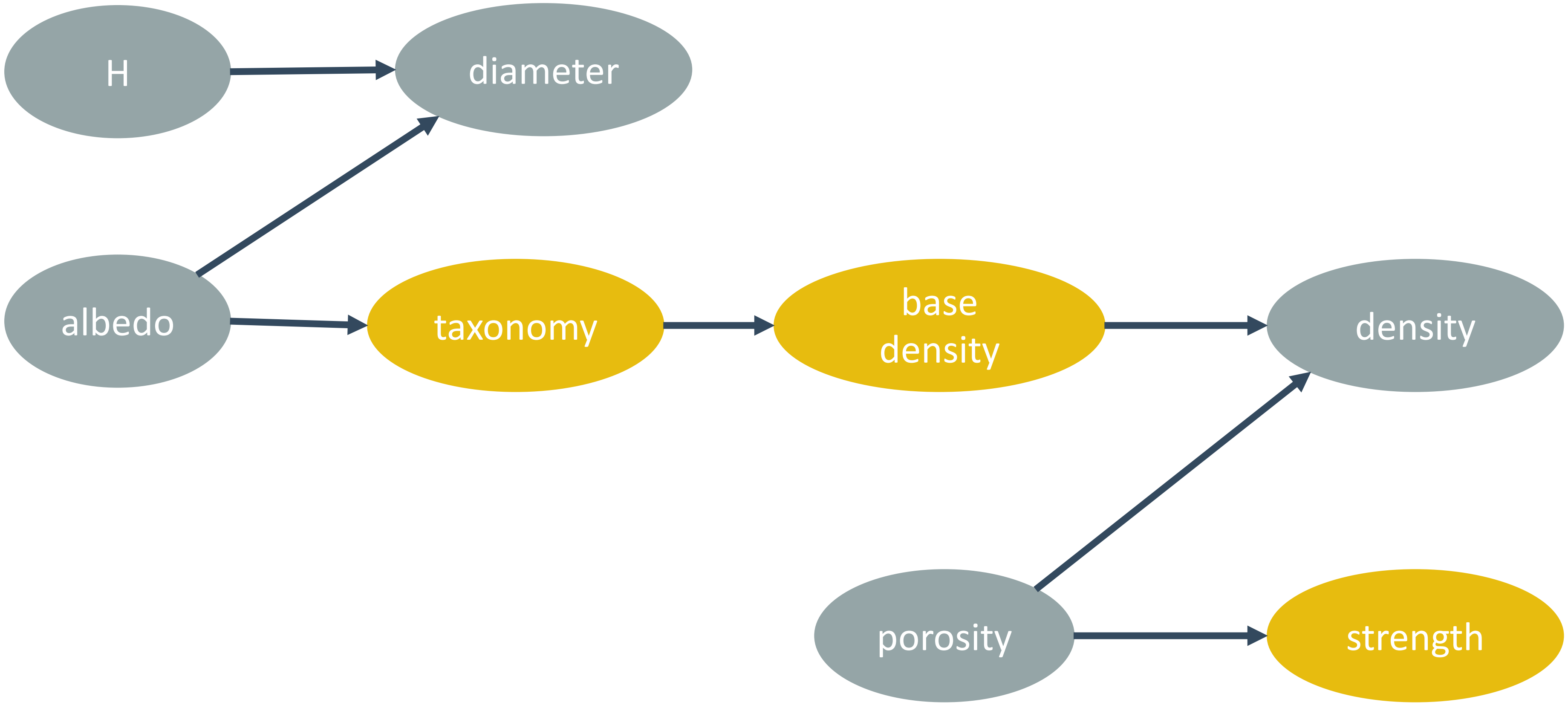

Asteroid Physical Property Inference Network

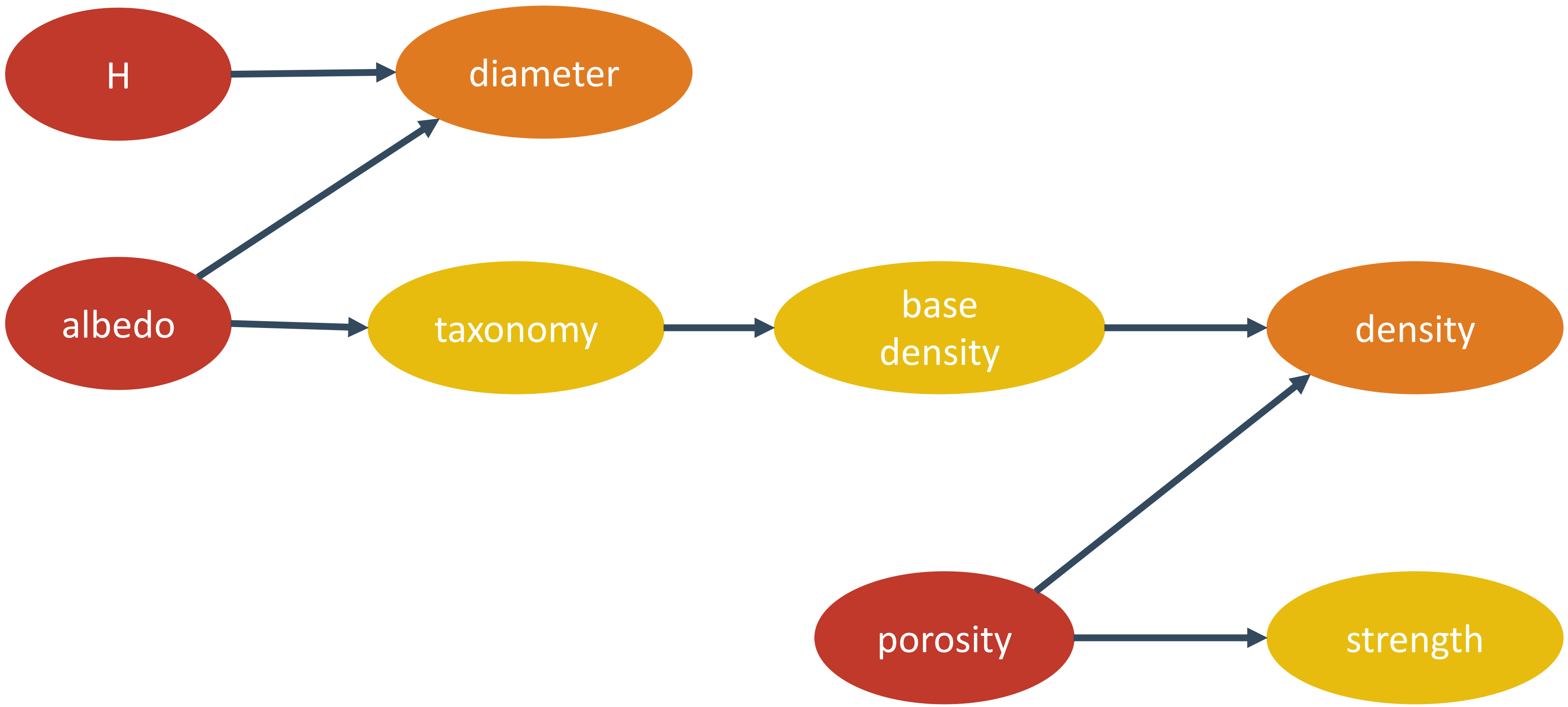

Taxonomy

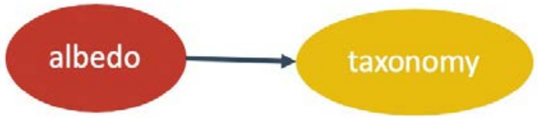

Taxonomy is inferred from albedo via Bayes Theorem

$$P(taxonomy|p_v) \sim P(p_v|taxonomy) * P(taxonomy)$$

albedo distribution for a specific taxonomy

frequency of taxonomy in the population

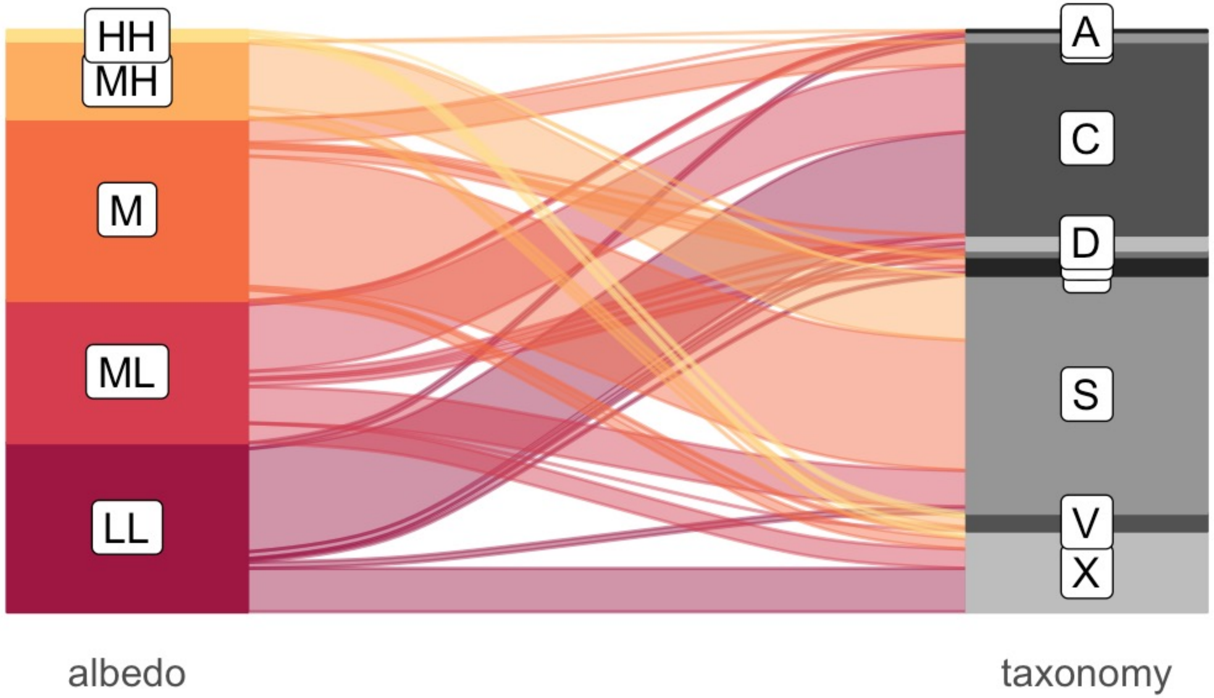

Base Density

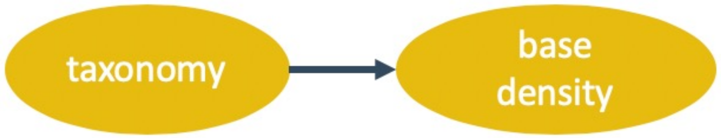

- A literature derived mapping was used to associate each taxonomy with related meteorites.
- Density measurements of meteorites were used to derive base density distributions for the associated taxonomy.
- Base densities were randomly selected from these distributions.

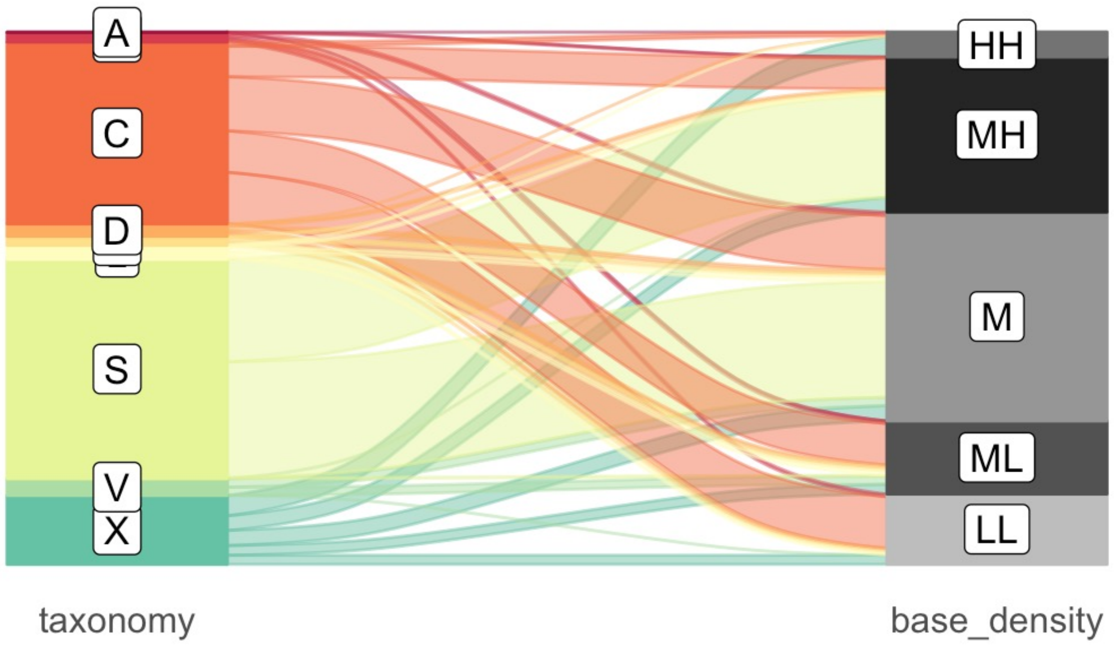

Aerodynamic Strength

- Strength values are selected from a uniform distribution in log space
- Virtual impactors in the lowest porosity quartile are randomly assigned a strength from the strongest quartile
- Other quartiles are mapped similarly

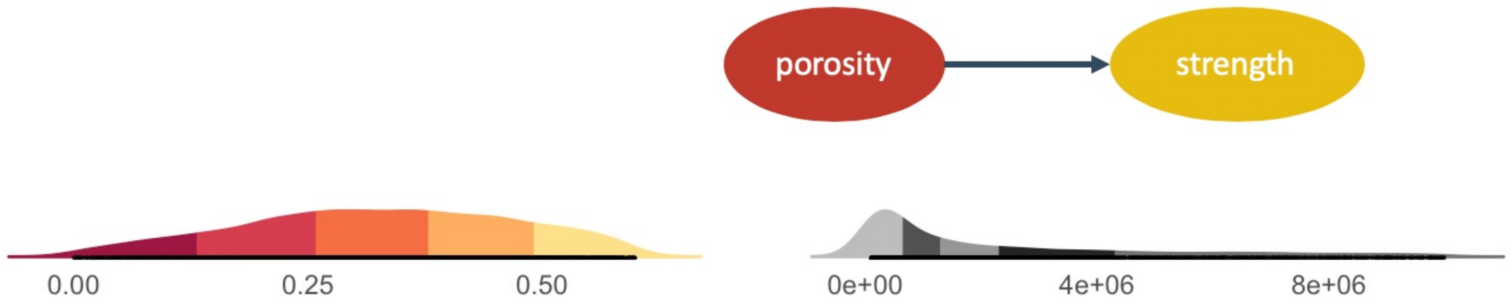

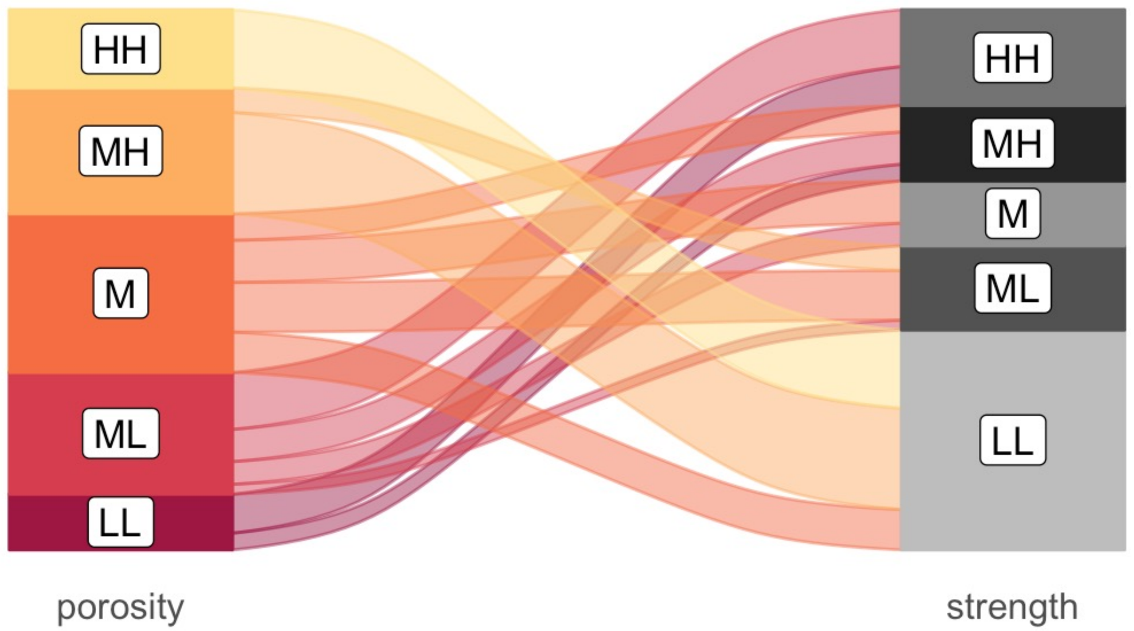

Asteroid Physical Property Risk Model Inputs

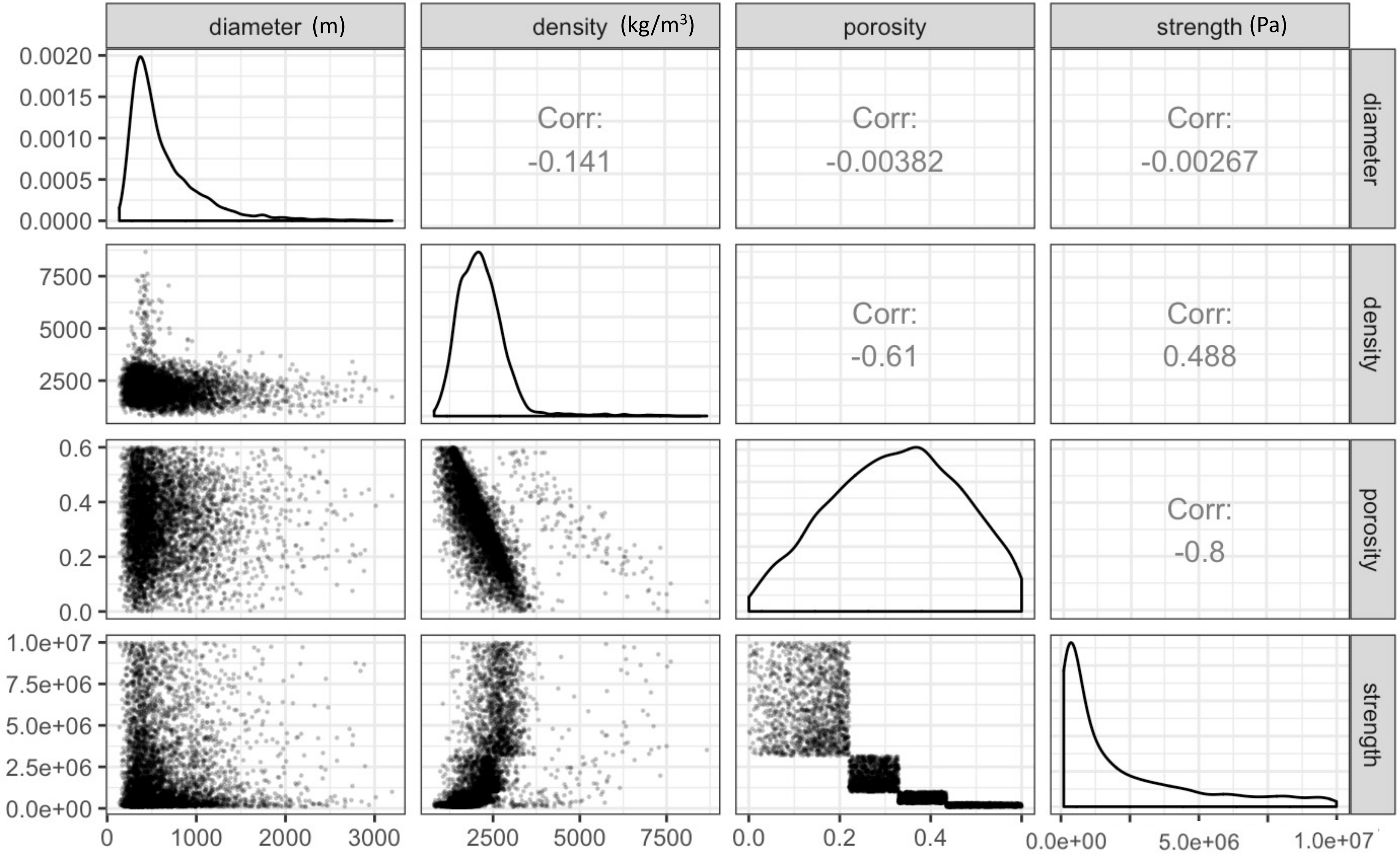

Characterization results can be incorporated into the inference network

Apophis Exercise Example:

- Used spectroscopy results
- Used NEOWise measurements
- Used radar measurements

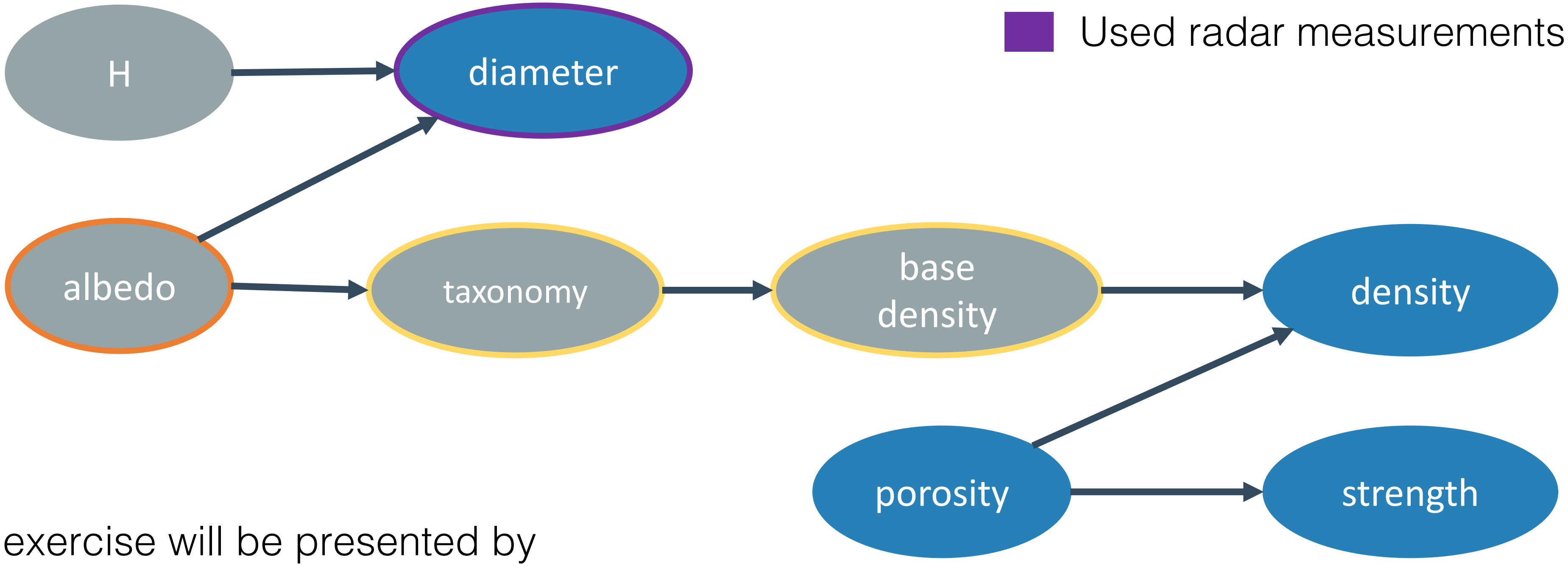

Apophis exercise will be presented by Kelley et al in session 13

Property distributions incorporate characterization observations

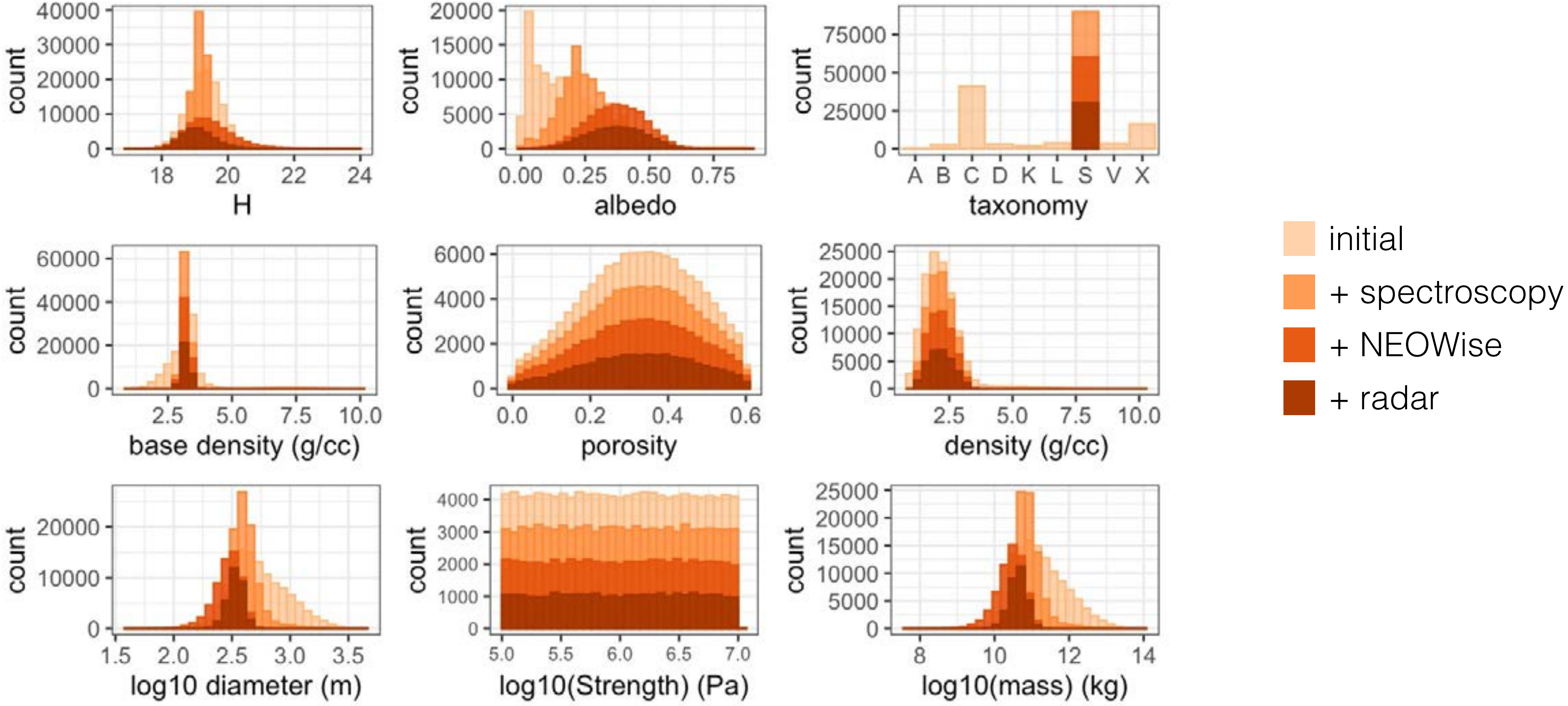

Local Damage Regions for different property sets

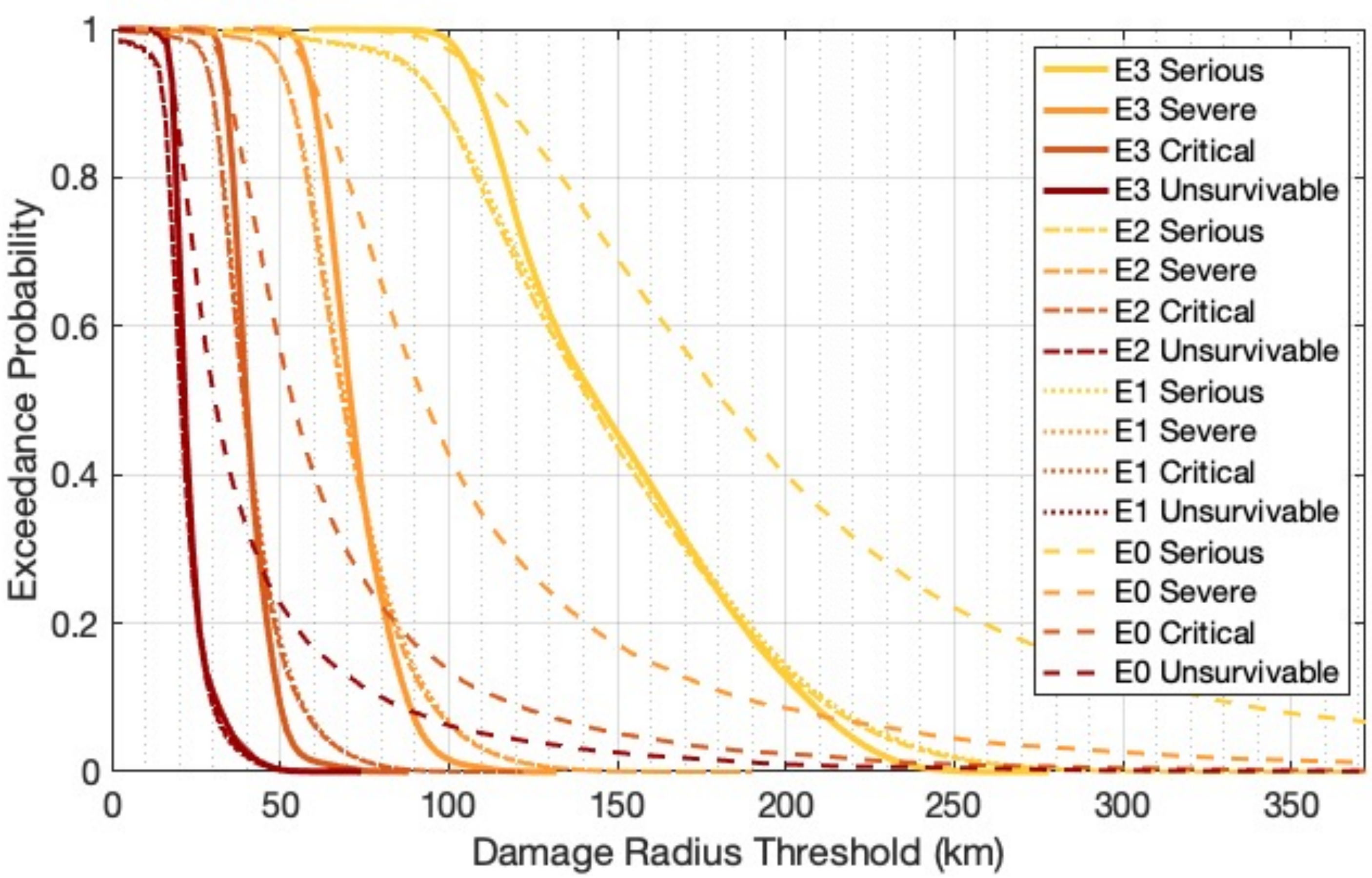

E0: initial
E1: + NEOWise
E2: + spectroscopy
E3: + radar

Physical Property Inference in Planetary Defense Scenarios

- Inference network simulates virtual impactors such that the distribution of their physical properties and the combination of these values for any impactor are physically plausible.
- The inference network has been used to support a variety of planetary defense exercises. (e.g. PDC, Apophis campaign)
- Future work includes improving inference nodes and improving ability to incorporate observational results.

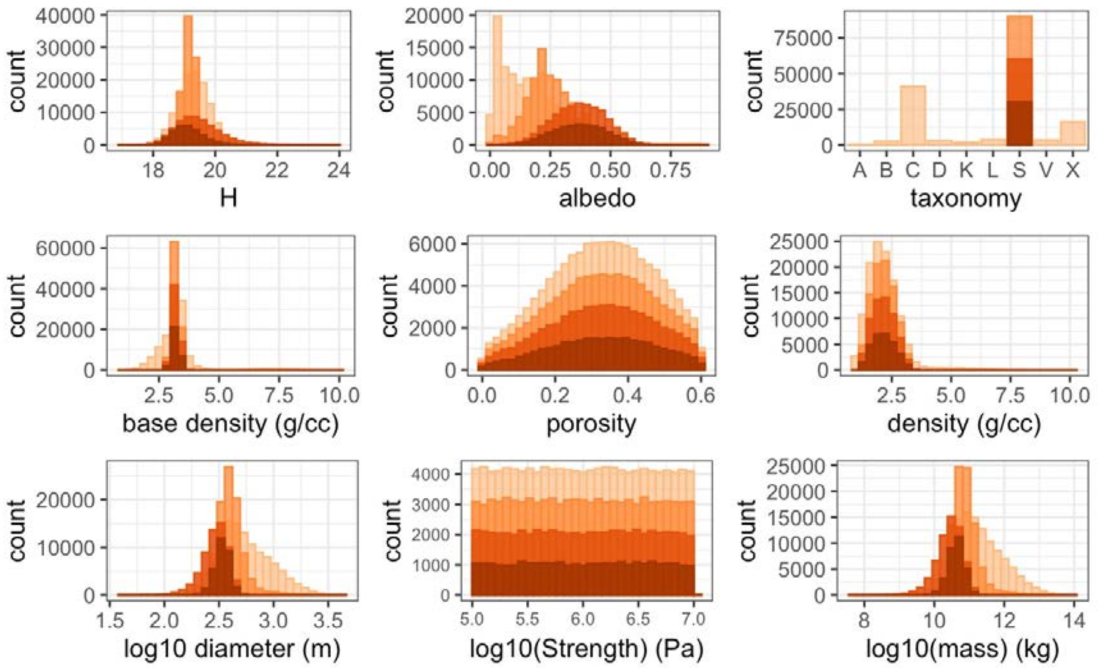

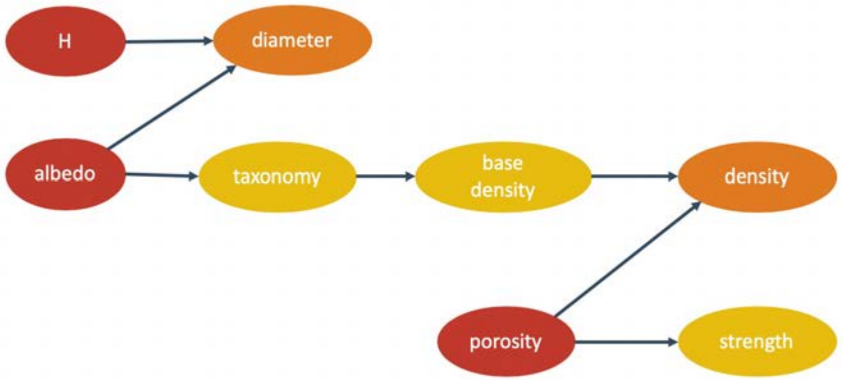

Ames Research Center

Meteorite Property References
Densities
Borovicka and Kalenda 2003; MaPS
Britt and Consolmagno 2003; MaPS
Britt and Consolmagno 2004; LPSC
Consolmagno and Britt 1998; MaPS
Hogan et al 2015; Icarus
Kohout et al 2014; Icarus
Li et al 2012; JGR
Macke 2010; Dissertation
Matsui et al 1980; Memoirs of National Institute of Polar Research
McCausland et al 2010; LPSC
McCausland et al 2007; MaPS
Opeil et al 2010; Icarus
Szurgot et al 2014; MetSoc
Wood 1963; The Solar System Vol. 4
Asteroid Property References
Mainzer et al 2016; NASA Planetary Data System
Carry 2012; PS&S
Asteroid to Meteorite Association References
Burbine et al 2002; Asteroids III
Burbine 2016; LPSC
DeMeo et al 2015; Asteroids IV
de Leon et al 2012; Icarus
Weisberg et al 1996; Geochemica et Cosmochimica Acta

7th IAA Planetary Defense Conference

26-30 April 2021, Online Event

Hosted by UNOOSA in collaboration with ESA

Q&A

Session 9b: Impact Effects

7th IAA Planetary Defense Conference

26-30 April 2021, Online Event

Hosted by UNOOSA in collaboration with ESA

Break

Up next: Session 10b - Disaster Management